The Thesis Committee for Mario Glikman
Certifies that this is the approved version of the following thesis:

Inclined Shear Reinforcement in Reinforced Concrete Slab-Column Connections

APPROVED BY
SUPERVISING COMMITTEE:

Supervisor: _____
Trevor D. Hrynyk

Co-Supervisor: _____
Oguzhan Bayrak

Inclined Shear Reinforcement in Reinforced Concrete Slab-Column Connections

by

Mario Glikman, B.E.

Thesis

Presented to the Faculty of the Graduate School of

The University of Texas at Austin

in Partial Fulfillment

of the Requirements

for the Degree of

Master of Science in Engineering

The University of Texas at Austin

May 2016

Dedication

A mi padre (†), por enseñarme que doctor se hace, pero señor se nace.

Acknowledgements

First of all, I would like to express my deepest gratitude to my advisor, Dr. Trevor Hrynyk, for the opportunity of being involved in the experimental research program since the beginning of the Master's program. His patience, comments, and constant encouragement have contributed to enhance my engineering and research skills. I would also like to thank Dr. Oguzhan Bayrak for taking the time to read this thesis. I am also grateful to all the laboratory staff and fellow students who helped and worked on such a challenging experimental program.

A huge part of this work is dedicated to all the wonderful people I met in Austin, who have made this two years of my life a very enjoyable experience. They include Mandy Chen, Stalin Armijos, Mauro Palavecino and his wife Lucia, Paul Biju-Duval and his wife Imy, Carine Choubassi, Alicia Bodas, Felipe Dias, Alex VanHout, and Felipe Sandoval.

My family and friends in Argentina also deserve to be deeply acknowledged for their constant support throughout my studies. I would like to thank my mother Ana María, my brother Pablo, my aunt Susy, and my sister-by-heart Natalia. I am also thankful to Horacio Pieroni, Roberto Príncipe, Francisco "Toti" Odeón, Mariano "Terra" Terraneo, German "El Negro" Caldeiro, Carla Tacchini, Javier "El Vasco" Darritchon, and María "El Mono" Hernández. Thank you all so much, this is yours more than mine.

I am grateful to the Bec.Ar Program for selecting me to pursue a master's degree in the US. This fellowship, founded by the Argentine President's Cabinet and the Buenos Aires Embassy of the United States and administered by the Argentinean Fulbright Commission, gave me the opportunity to accomplish one of my biggest life's milestones, to study abroad.

Last but not least, I would like to thank Lucrecia for her love, encouragement, and unconditional support. Despite the physical distance over the course of my studies, I felt she was alongside me all the time. Thank Lucre so much for showing me that is possible to bridge the gap between engineering and arts. I love you.

Abstract

Inclined Shear Reinforcement in Reinforced Concrete Slab-Column Connections

Mario Glikman, M.S.E.

The University of Texas at Austin, 2016

Supervisor: Trevor D. Hrynyk

Co-Supervisor: Oguzhan Bayrak

Reinforced concrete flat slabs are widely used in modern infrastructure. Due to their comparatively simple construction, flat slabs have become especially prevalent in mid- to high-rise buildings. The performance of slab-column connections has been critically studied over the last several decades by researchers aiming to better understand the behavior of flat slabs subjected to punching shear loading conditions. As a result, the use of slab shear reinforcement has emerged as a practical strategy to improve both the strength and ductility of reinforced concrete flat slabs.

The primary objective of this research study was to investigate the behavior of reinforced concrete slab-column connections employing a novel shear reinforcement system consisting of inclined deformed steel reinforcing bars. Results are presented from an experimental program conducted at the Ferguson Structural Engineering Laboratory of The University of Texas at Austin. The results show that a premature failure attributed to inadequate shear reinforcement anchorage controlled the performance of the strengthened slabs. Lastly, a study of the bond stress development in the slab shear reinforcement was

carried out to investigate whether this anchorage-driven failure can be captured using different provisions currently available for the assessment of reinforced concrete flat slabs.

Table of Contents

List of Tables

List of Figures

Chapter. 1 Introduction

1.1 BACKGROUND

Reinforced concrete (RC) flat slab systems are widely used in modern building infrastructure. Historically, these types of structures employed large transitioning capitals, often conical, to facilitate the flow of forces from the slab to the supporting columns. In recent decades, flat slabs without capitals (i.e., flat plate systems) have become much more prevalent, mainly due to efficiencies associated with their simpler forms and reduced construction requirements. However, in contrast to their simple forms, the load transfer mechanisms involved in flat plates can be rather complex. Three-dimensional loading conditions consisting of combined flexure and shear often lead to increased load resistance demands, particularly in regions forming slab-column connections.

1.2 MOTIVATION AND OBJECTIVES

Among the primary objectives in the design of two-way reinforced concrete slab systems is the requirement to mitigate and/or prevent the onset of premature brittle punching shear failures. Such undesirable failure modes have been shown to occur in flat plates that have been exclusively reinforced in their planar directions and, in several instances, have been deemed responsible for the onset of total structure failure (Mitchell and Cook, 1984).

In that light, this thesis presents the findings from an experimental testing program conducted at the Ferguson Structural Engineering Laboratory of The University of Texas at Austin aimed toward investigating the usage of a novel slab shear reinforcement assembly for slab-column connections. The novel reinforcing assembly is comprised of an assembly of inclined deformed bars in a stirrup-like configuration. The

efficacy of the novel shear reinforcing assembly was evaluated experimentally by way of a series of large-scale RC slab-column connections subjected to concentric loading conditions. Additionally, an analytical study was carried out to evaluate the adequacies of various codes of practice in estimating the two-way shear strength of RC slab-column connections. Merits and limitations associated with different codes of practice are also presented.

1.3 ORGANIZATION

The second chapter of this thesis provides relevant background information that has been organized into two categories: (i) an overview of several relevant prior research programs that have been conducted to investigate the performance of RC members constructed with inclined shear reinforcement, and (ii) a summary of several codes of practice that are available for two-way shear design of RC slab-column connections.

Chapter 3 documents the experimental program, summarizing the slab-column connection details, the instrumentation and data measurement techniques employed, and the testing procedures employed in the experimental program.

Test observations and an overview of the key results obtained from the experimental testing program are presented in Chapter 4.

Analysis and discussion pertaining to the main findings of the experimental program are presented in Chapter 5. Additionally, estimates of shear capacities provided by codes of practice are also presented in this chapter.

Lastly, Chapter 6 summarizes the key findings from the testing program and conclusions regarding the slab strength estimates provided by the different code provisions considered.

Chapter. 2 Literature Review

A large volume of experimental research has been performed in an effort to better understand the formation of, and to develop strategies to mitigate, brittle punching shear failures in RC flat slabs. The vast majority of these types of research investigations have focused on assessing the shear resistance of flat plate slab-column connections constructed without through-thickness shear reinforcement. With few exceptions, studies dedicated to investigating the performance of RC flat slabs containing inclined shear reinforcement are essentially absent from the current database of literature. Consequently, studies focused on investigating the influence of inadequate anchorage on the effectiveness of shear reinforcement in RC flat slabs are also scarce.

This chapter summarizes a review of relevant literature and is approached from two viewpoints: Section 2.1 summarizes a series of research investigations aimed toward investigating the performance of RC members constructed with inclined shear reinforcement and illustrating the importance of adequate reinforcement anchorage in providing effective through-thickness shear reinforcement. Section 2.2 provides a brief summary of codes of practice that are typically used to design and estimate the punching strength of shear-reinforced flat slabs. Lastly, a summary of the main findings attained from the literature and design procedure review is presented in Section 2.3.

2.1 USE OF INCLINED SHEAR REINFORCEMENT

2.1.1 Richart (1927)

Over the course of approximately 12 years, Richart conducted a series of testing programs to study the performance of various forms of shear reinforcement and to gain improved understanding on the distributions and levels of stress developed in such shear

reinforcing elements. In total, 139 RC beams were tested over a period from 1910 to 1922. The beams comprising the program were used to investigate different web reinforcement arrangements: both loose and rigidly attached/anchored vertically oriented stirrups, inclined stirrups welded to the longitudinal bars, unit frames, bent-up bars, and various combinations of these different types of web reinforcement.

The findings of the investigation showed that, as a result of welding web reinforcement to longitudinal bars, the reinforcement was capable of developing full strength. It was noted that preventing the slipping of stirrups at their ends was a key parameter to the effectiveness of this reinforcement. Furthermore, Richart suggested that properly designed anchors and/or hooks seemed to be a reasonable method of improving the effectiveness of through-thickness shear reinforcement. Also of interest, it was noted that inclined stirrups were shown to develop appreciable stress levels at lower load in comparison to vertically oriented shear reinforcement. Lastly, it was found that RC beams reinforced with inclined shear reinforcement, placed at larger longitudinal spacing increments, achieved shear capacities similar to those obtained by RC beams employing vertically oriented reinforcement with reduced longitudinal spacing.

2.1.2 Oliveira et al. (2000)

Oliveira et al. carried out an experimental program aimed toward investigating the efficiency of a novel form of inclined stirrups. Eleven model RC slabs of 1/2 to 2/3 scale were tested. Two slabs were constructed without shear reinforcement, three contained conventional vertical stirrups that were placed orthogonally from the column faces, and five slabs were constructed with inclined through-thickness reinforcing members, with inclination angles of 57 degrees from the longitudinal axis.

Results from the investigation showed distinctly better performance for the slabs containing inclined stirrups relative to those constructed with vertical stirrups. The authors suggested that inclined stirrups can be an effective way to shear strengthen flat plate slabs. In addition, this particular form of reinforcement was noted to be easy to install, as the inclined shear reinforcing members could be placed after all longitudinal reinforcement was positioned.

2.1.3 Beutel and Hegger (2002)

Beutel and Hegger performed an experimental testing program consisting of ten RC slab punching tests with conventional stirrups and stirrups made of fabric reinforcement. Isolated RC slab-column connections were subjected to an upward monotonically increasing load and were restrained vertically at twelve points using high-strength tie rods. The restraints were positioned in an attempt to simulate the structural response of critical slab-column connection regions. In addition to the experimental work, three-dimensional finite element simulations were performed to investigate the effectiveness of different anchor types: straight links, anchored links by 90-, 135-, and 180-degree bends, transverse welded bars, headed anchors, and several different combinations of these elements.

Both the experimental program and the numerical simulations showed that the anchor types strongly influenced the effectiveness of the shear reinforcement: the straight link, anchored only by bond, developed the lowest steel stress. The 180-degree bend without enclosing a longitudinal bar reached the same stress level of that of the 90-degree bend. The maximum link stress was reached by a 180-degree bend that enclosed longitudinal reinforcement. However, transverse welded bars significantly improved the anchorage qualities. The authors noted that stirrups did not have to enclose the bottom

mat of flexural reinforcement, provided they were welded to longitudinal horizontal runners.

2.1.4 Muttoni et al. (2010)

The research performed by Muttoni et al. involved an investigation on the use of inclined post-installed shear reinforcement as a means of strengthening flat plate RC slab-column connections. The retrofit solution involved the use of a series of steel bars, doweled and bonded within an existing RC slab using high-performance epoxy adhesive. The inclined reinforcing bars were installed in holes that were drilled into the soffit of the slab-column connection. A series of 12 RC slabs with post-installed rods were tested under concentric punching shear loading conditions to investigate the suitability of the proposed retrofit.

Results from the testing program showed that the addition of the inclined shear reinforcing members in the slab-column connections led to significant increases in both strength and deformation capacity relative to that of slabs without shear reinforcement. Note that, in this case, the use of inclined bars was specifically selected as it led to increased anchorage lengths of the epoxy-bonded reinforcing bars. The authors noted that the capacity and rotation of the specimens was strongly influenced by the amount of shear reinforcement and the longitudinal reinforcement ratio.

2.2 PROVISIONS FOR ESTIMATING THE SHEAR STRENGTH OF TWO-WAY SLABS

Four sets of provisions are analyzed in this section: ACI 318-14, *fib* Model Code 2010, Eurocode 2, and the Critical Shear Crack Theory (CSCT) (Muttoni et al., 2009). A brief description of each of the four procedures is presented herein along with the assumptions used inherently in the determination of the punching shear strength of flat

slabs. Additional details pertaining to the usage of the provisions are presented in Appendix A.

2.2.1 ACI 318-14 (Building Code Requirements for Structural Concrete)

A common approach for estimating the punching shear strength of flat RC slabs containing shear reinforcement is based on the assumption that the slab shear resistance can be subdivided into the resistance provided by concrete and, if present, the resistance provided by shear reinforcement. In evaluating the punching shear strength of a two-way flat slab, ACI 318-14 recommends that the critical section requiring examination be located so that its perimeter b_0 is at least, but need not approach closer than, the distance of $d/2$ measured from the column face (refer to Figure 2.1), where d is the distance from the centroid of the tensile reinforcement mat to the soffit of the slab. In addition, the provisions of ACI 318-14 are developed on the basis of a 45-degree truss model and, as such, the critical crack occurring from the soffit of the slab near the column is assumed to occur at an angle of 45 degrees measured between the crack and the slab plane.

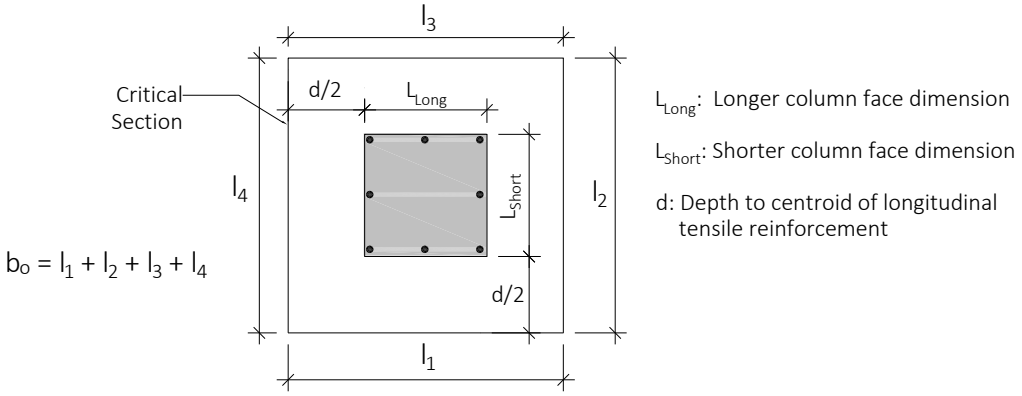

Figure 2.1: Critical section defined by ACI 318-14 (Adapter from ACI 318-14, 2014)

ACI 318-14 limits the nominal shear strength as well as the concrete contribution depending on the type of shear reinforced system employed. It is worth noting that the

permissible shear resistance is not a function of the depth of the slab. As such, the ACI 318-14 does not consider size effect. Additionally, the influence of coexisting stresses attributed to flexural bending moments or the ratios of longitudinal reinforcement are not explicitly considered in these provisions.

2.2.2 *fib* Model Cole 2010 (Model Code for Concrete Structures)

As is the case in ACI 318-14, *fib* Model Code 2010 considers a critical perimeter section (b_0) located at a distance of $d_v/2$ measured from the column face, where d_v, the shear-resisting depth of the slab, is the distance from the centroid of the tensile reinforcement layers to the centroid of the longitudinal compressive force resultant, with a 45-degree angle for the critical crack (see Figure 2.2).

Following the approach outlined in ACI 318-14, the punching shear strength is taken as the summation of the resistance provided by the concrete and the resistance provided by the shear reinforcement.

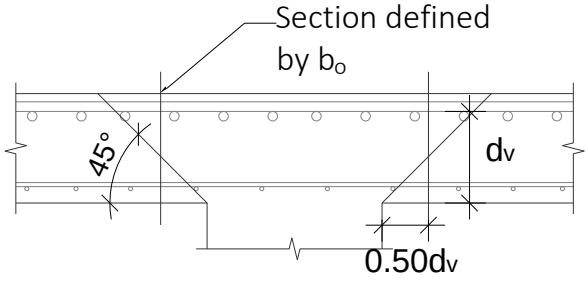

Figure 2.2: Critical section defined by *fib* 2010, schematic cross section (Adapted from *fib* Model Code 2010)

There are three interesting points to note when comparing the provisions of ACI 318-14 to those of *fib* 2010: (1) The punching shear resistance specified by the *fib* Model Code is influenced by the maximum nominal aggregate size of the concrete, (2) *fib* establishes that the punching shear capacity is dependent on slab rotation, and (3)

according to *fib*, the strength provided by the shear reinforcement is dependent on the bond stress of the shear reinforcement. Note that ACI 318-14 assumes full yield of shear reinforcement with no explicit consideration for the bond stress development or anchorage.

2.2.3 Eurocode 2 (Design of Concrete Structures)

The Eurocode 2 design procedure for RC slab punching is based on checks at a series of control sections, defined by their control perimeters. The basic control perimeter u_1 is normally taken at a distance $2d_{eff}$ from the loaded area and is constructed to minimize its length (see Figure 2.3). As defined in both ACI 318-14 and *fib* Model Code 2010, the punching shear capacity is treated as the summation of the shear resistance provided by concrete and the resistance provided by the shear reinforcement.

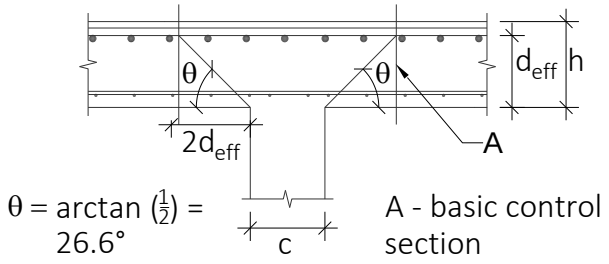

Figure 2.3: Verification model for punching shear at ULS (Adapted from Eurocode 2, 2004)

2.2.4 The Critical Shear Crack Theory (CSCT)

The Critical Shear Crack Theory (CSCT) is a theoretical model based on the assumption that punching shear failure occurs due to the opening of a critical shear crack, as shown in Figure 2.4. In this case, a fraction of the applied load is carried by concrete (the ability of carrying the load is limited by the opening of the crack and by its roughness), while the rest of the shear force is assumed to be resisted by shear reinforcement.

According to this theory, the concrete contribution is estimated from the assumption that the critical shear crack develops within a 'failure zone'. The contribution of the shear reinforcement is determined using the main hypothesis of this theory, which states that the width of the critical shear crack is proportional to the product of the effective depth of the specimen times the rotation of the slab.

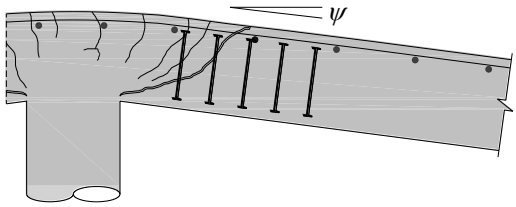

Figure 2.4: Localization of the strain at failure zone (Adapted from Muttoni et al., 2009)

In this model, the width of the critical shear crack is correlated to the rotation of the slab. As described, note that the CSCT behavioral model accounts for size effect as well as for softening due to the slab deformation. Taking advantage of the compatibility relations introduced by the CSCT, the contribution of concrete and steel to resist shear forces can be estimated using mechanical and geometrical parameters.

2.3 SUMMARY

A general synopsis of the previous studies is listed below:

- RC flat slabs containing inclined shear reinforcement have shown to outperform slabs containing vertically oriented through-thickness reinforcement in terms of both strength and deformation capacity.
- A key parameter affecting performance of through-thickness shear reinforcement is member anchorage. Codes of practice and former research investigations encourage the application of detailing rules to ensure adequate anchorage. For

example, many building codes require that stirrups enclose the top and the bottom mats of flexural reinforcement (ACI 318-14, Eurocode 2). Additionally, transverse members welded to horizontal runners, especially at the bottom longitudinal reinforcement, have demonstrated significant improvement in the anchorage of shear reinforcement.

- All studied provisions approach the calculation of the punching shear capacity of reinforced concrete flat slabs by determining the shear resistance provided by concrete plus the shear capacity provided by the shear reinforcement. However, there are differences amongst the specifications, specifically in the way that the punching shear strength is calculated. ACI 318-14 seems to follow the most straight-forward method of designing for punching shear. There is no explicit consideration of the bond stress development in the shear reinforcement. As such, it does not provide any formulation to determine the value of the working stress of the shear reinforcement. CSCT, on the other hand, does consider the bond strength as a key element for the determination of the shear capacity of the shear reinforcement. *fib* 2010 Model Code is a code-like formulation of CSCT. Thus, a procedure similar to that of the CSCT needs to be carried out to estimate the punching shear capacity of flat slabs. For further details regarding the calculation processes, refer to Appendix. A.

Chapter. 3 Experimental Program

An experimental program consisting of four full-scale RC slab-column connections under concentric punching shear loading conditions was performed at The Ferguson Structural Engineering Laboratory (FSEL) at The University of Texas at Austin. The testing campaign was developed to investigate the performance of RC slab-column connections employing a novel shear reinforcement system consisting of inclined deformed steel reinforcing bars.

In this chapter, the structural details and procedures used to construct the slab-column connections are presented in Section 3.1. Material properties for the steel reinforcement and concrete comprising the specimens are summarized in Section 3.2. Section 3.3 contains the details of the test setup and instrumentation. Lastly, Section 3.4 closes the chapter with an overview of the test procedure used in the testing program.

3.1 TEST SPECIMENS

The primary goal of the testing program was to evaluate the performance of a novel slab shear reinforcement assembly. To do so, the four slab-column connections summarized in Table 3.1 were tested. With the exception of the different shear reinforcement systems/configurations employed, the specimens were designed to be nominally identical in all aspects.

Table 3.1: Experimental Program Specimens Matrix

Specimen	ρ_l	ρ_v [e]	A_v [a]
Slab 1	1.60 %	0.41 %	Studs [b]
Slab 2	1.50 %	0.34 %	Inclined bars [c]
Slab 3	1.50 %	0.51 %	Inclined bars [d]
Slab 4	1.40 %	-	-

[a] Area of shear reinforcing steel per column face
[b] 2 vertical studs (A_v = 0.20 in.^{2} (130 mm^2)) equally spaced at 4.0 in. (100 mm) longitudinal spacing
[c] 4 inclined bars at 35 degrees. Av = #3 equally spaced at 7.5 in. (190 mm) longitudinal spacing
[d] 4 inclined bars at 35 degrees. Av = #3 variably spaced from 5.0 in. (130 mm) to 10.0 in. (250 mm) longitudinal spacing
[e] Shear reinforcement ratio pertaining to critical section located at d/2 from column face

3.1.1 Details of the Novel Shear Reinforcing Assembly

Two types of shear reinforcement were used: (1) a commercially available shear stud rail system consisting of smooth steel studs that are end-anchored to the concrete by way of anchor heads and welded steel rails, and (2) a novel shear reinforcing system comprised of an assembly of bent No. 3 weldable rebars (Grade 60) in a stirrup-like configuration which are anchored at the base of the slab to steel horizontal runners. The tops of the inclined members are bent in a hooked configuration to provide anchorage, and to limit interference with in-plane reinforcing bars (refer to Figure 3.1).

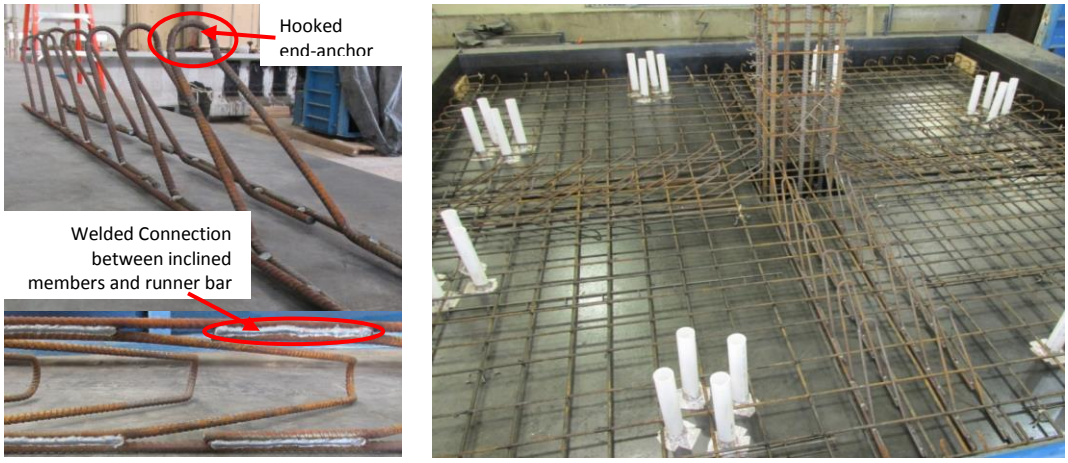

(a) (b)

Figure 3.1: Novel Shear Reinforcing System; (a) Assembly, (b) As positioned in Slab 2

A detailed drawing of the inclined working members comprising the novel shear reinforcing assembly is presented in Figure 3.2.

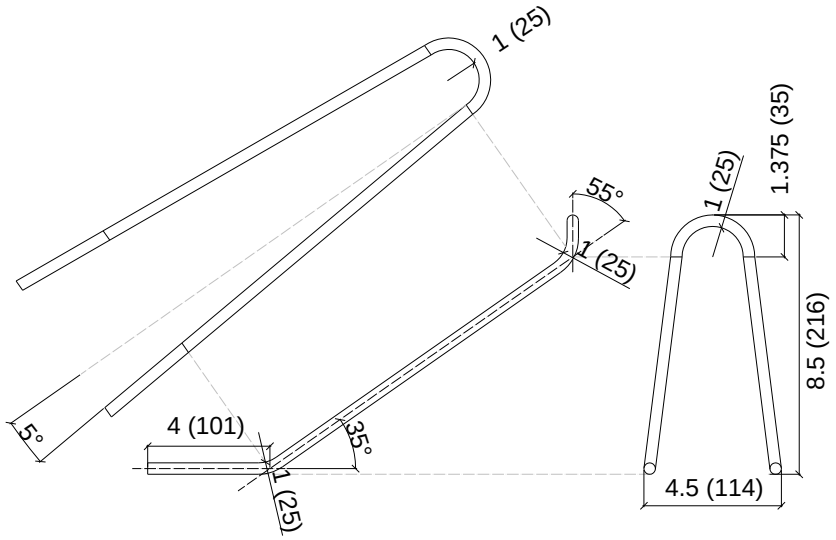

Figure 3.2: Inclined Working Member Geometry; Novel Shear Reinforcing System [in. (mm)]

3.1.2 Specimen Details

The four slab-column connections were nominally identical in terms of geometry, in-plane reinforcement composition, and concrete material strength. The shear reinforcement comprising the four specimens served as the primary testing variable: one slab-column connection was constructed with the novel inclined shear reinforcement system with equally spaced inclined bars (i.e., working members), one specimen was constructed using the novel shear reinforcement system employing variable working member spacing, one specimen was constructed using conventional vertically-oriented headed steel studs, and one slab-column connection was constructed with no shear reinforcement, serving as the control specimen.

The test specimens were 12 ft. (3.5 m) square, had 10 in.–thick slabs (250 mm-thick), and were monolithically constructed with 16 in.-square intersecting columns (400 mm-square). The slabs contained two mats of in-plane reinforcement with ratios of approximately 1.50 % on the tension side and 0.20 % on the compression side. A clear cover of 0.75 in. (19 mm) was provided for the slab. The columns were constructed with a longitudinal reinforcement ratio of 1.90 %. All of the assemblies were designed such that punching shear failure would occur prior to yielding of the flexural reinforcement. Figure 3.3, Figure 3.4, and Table 3.2 summarize of the main characteristics of the specimens.

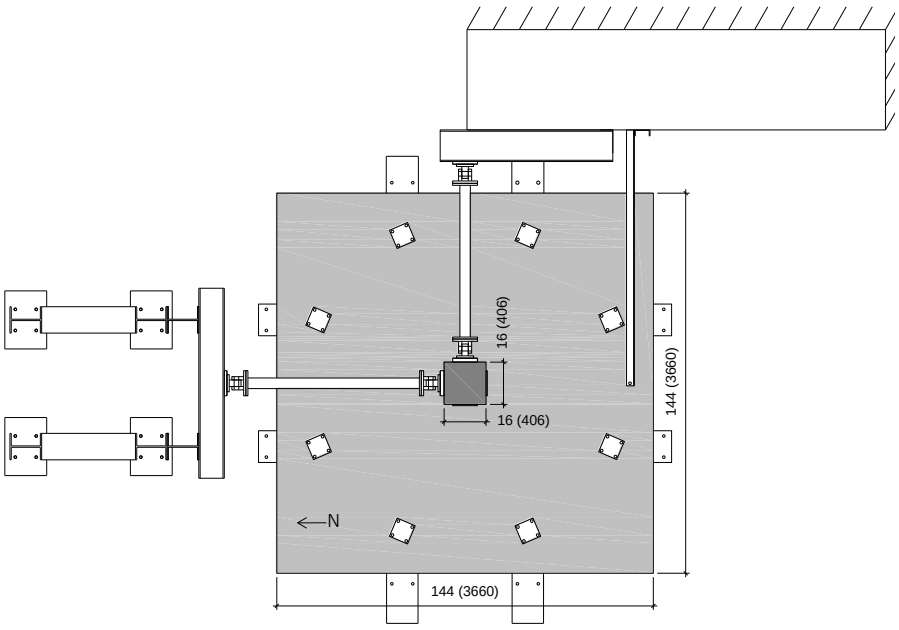

Figure 3.3: Specimen Geometry; Plan View [in. (mm)]

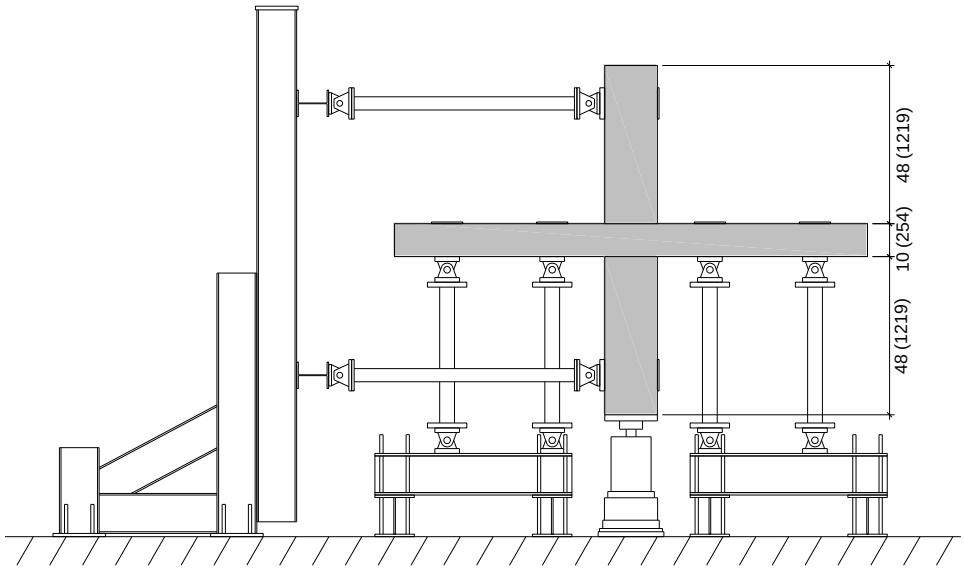

Figure 3.4: Specimen Geometry; West Elevation [in. (mm)]

Table 3.2: Test Specimens; Slab Reinforcement

Slab	Longitudinal					Shear			
	Mat	Size	Ave Sp. [in. (mm)]	Max Sp. [in. (mm)]	Min Sp. [in. (mm)]	Type	Ave Sp. [in. (mm)]	Max Sp. [in. (mm)]	Min Sp. [in. (mm)]
1	Top	US#7	4.25 (108)	5.0 (127)	3.5 (89)	Stud	4.0 (100)	4.0 (100)	4.0 (100)
	Lower	US#3	5.5 (140)	6.0 (152)	5.0 (127)				
2	Top	US#7	4.25 (108)	5.0 (127)	3.5 (89)	Incl.	7.5 (190)	7.5 (190)	7.5 (190)
	Lower	US#3	5.5 (140)	6.0 (152)	5.0 (127)				
3	Top	US#7	4.25 (108)	5.0 (127)	3.5 (89)	Incl.	7.5 (190)	10.0 (254)	5.0 (127)
	Lower	US#3	5.44 (139)	6.0 (152)	4.87 (124)				
4	Top	US#7	5.0 (127)	6.0 (152)	4.0 (100)	-	-	-	-
	Lower	US#3	4.5 (114)	5.5 (140)	3.5 (89)				

The designs of the shear-reinforced slab assemblies were done according to ACI 318-14. As shown in Figure 3.5, Slabs 1 and 2 were designed to achieve equal shear resistance provided by the shear reinforcement (i.e., equal V_s). However, Slab 3, was designed such that it contained the same total volume of shear reinforcement, but was proportioned using a variable longitudinal spacing. This was done in an effort to maximize the shear resistance provided by the inclined reinforcing assembly near the column, where the shear stresses are greatest, and punching failures typically occur. Note that the nominal yield strength of the smooth studs was 63 ksi (435 MPa), whereas the nominal yield strength of the No. 3 deformed bars was 78 ksi (536 MPa). Figure 3.5 also presents the average shear reinforcement per unit length for each slab (i.e., χ), calculated as follows:

$$\chi = \frac{\sum A_v \left(\sin\alpha + \cos\alpha\right)}{\sum s} \tag{3-1}$$

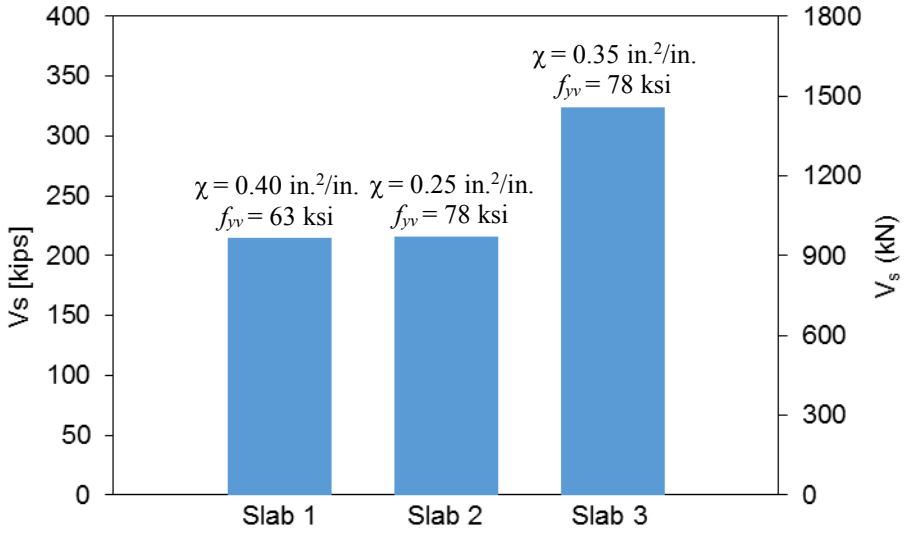

Figure 3.5: Shear Strength Provided by Shear Reinforcement According to the Provisions of ACI 318-14

3.2 MATERIAL PROPERTIES

3.2.1 Concrete

Ready-mix concrete with a nominal maximum course aggregate size of 1 in. (25.4 mm) limestone, and a target cylindrical compressive strength of 4 ksi (27.6 MPa) was used. Table 3.3 presents a summary of the mechanical property tests carried out, and the ages of specimens at the time of testing. Additional results obtained from concrete material testing are provided in Appendix. B.

Table 3.3: Concrete Mechanical Properties

Slab	f'_c [a] [psi (MPa)]	Age [Days]	E_c [ksi (MPa)]	ε'_c $x10^{-3}$	f'_t [b] [psi (MPa)]	f_r [c] [psi (MPa)]	f_{ct} [d] [psi (MPa)]
1	4,180 (28.8)	107	4,890 (33720)	-1.706	416 (2.87)	644 (4.44)	447 (3.08)
2	4,190 (28.9)	38	3,720 (25650)	-1.522	370 (2.55)	715 (4.93)	453 (3.12)
3	3,900 (26.9)	25	3,450 (23790)	-1.896	403 (2.78)	606 (4.18)	340 (2.34)
4	3,260 (22.5)	33	3,220 (22200)	-1.578	309 (2.13)	606 (4.18)	389 (2.68)

[a] Compressive Strength Test (ASTM C39)
[b] Direct Tension Test (No test standard available)
[c] Modulus of Rupture Test (ASTM C78)
[d] Split Tension Test (ASTM C496)

3.2.2 Steel Reinforcing Bars

The mechanical properties of the steel reinforcement provided in the RC slabs are presented in Table 3.4. The results presented were obtained from testing three coupons for the weldable bars and five tests for all other steels.

Table 3.4: Mechanical Properties of Steel Reinforcing Bars

Type of Reinforcement	Designation	Average Yield Strength [ksi (MPa)]	E_s [ksi (MPa)]	Average Ultimate Strength [ksi (MPa)]
Longitudinal [e]	No.3	77.0 (531)	28610 (197260)	120.1 (828)
	No.7	73.5 (507)	27580 (190160)	107.1 (738)
Shear Studs [f]	½" headed	61.8 (426)	30710 (211740)	77.6 (535)
Shear Inclined Bars [g]	No.3	77.1 (532)	29340 (202290)	98.4 (678)

[e] Grade 60 deformed reinforcing bars
[f] Grade 60 smooth steel studs
[g] Grade 60 weldable deformed reinforcing bars

3.3 DETAILS OF TEST SETUP

Figure 3.6 shows a schematic plan of the test setup, while Figure 3.7 presents a perspective view of the test setup.

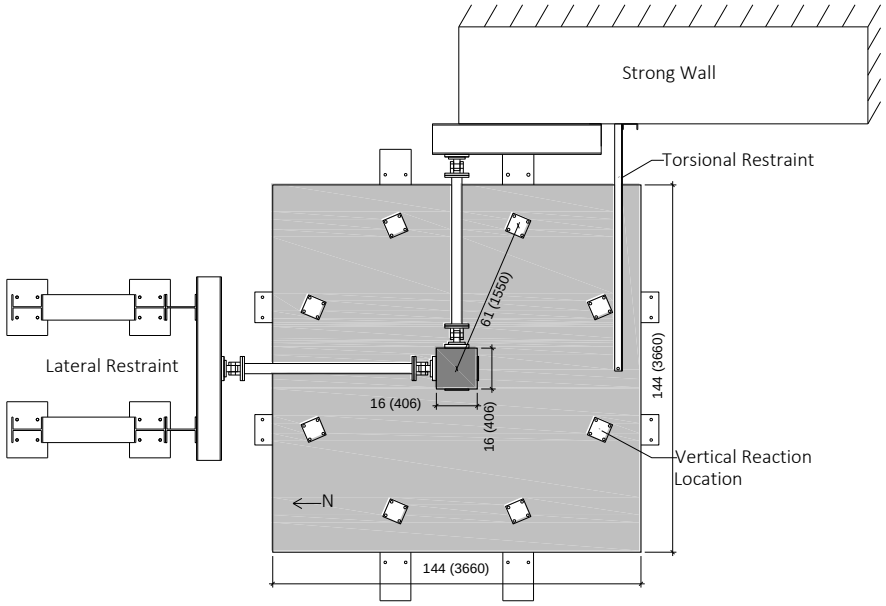

Figure 3.6: Test Setup; Plan View [in. (mm)]

Figure 3.7: Test Setup; Perspective view

An upward monotonically increasing load was applied to the lower column to produce concentric shear loading conditions. Eight pin-pin-connected vertical struts were positioned along the perimeter of the slab to serve as restraints. The struts were positioned in a circular restraint pattern with a diameter of 61 in. (1.5 m), resulting in an average a/h ratio (shear span-to-slab height ratio measured from the face of the column) of approximately 5. The circular restraint pattern provided equal support-to-column shear spans amongst the struts. To ensure that the specimens remained stable, a lateral support-frame was provided. Figure 3.8 provides additional details of the support assembly.

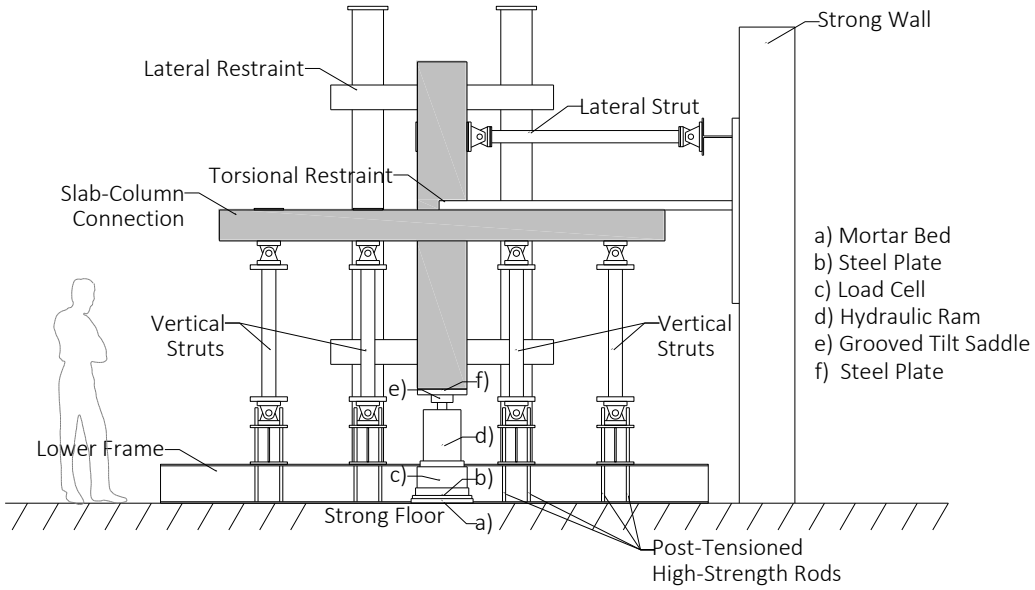

Figure 3.8: Test Setup Details; North Elevation

3.3.1 Specimen Instrumentation

The RC slab assemblies were well-instrumented. Electrical resistance strain gages were attached to in-plane and out-of-plane steel reinforcement. The placement of the strain gages was done to obtain representative steel strain measurements to be used for further analysis. The applied load on the column was measured using a 1,000,000 lb (4450 kN) load cell placed between the hydraulic ram and the concrete strong floor (refer to Figure 3.8). Load cell measurements were verified using hydraulic pressure measurements from the pump. Vertical displacements were measured at various locations of the slab using linear potentiometers (LPOTs). LPOTs were installed beneath the slab, and their placement was established to obtain representative slab deflections and rotations. All instrumentation was connected to a data acquisition system, and data were recorded simultaneously using a sampling rate of approximately 0.30 Hz.

3.4 TEST PROCEDURE

Prior to performing each test, all instrumentation was checked to ensure proper functionality. To facilitate this verification, a preload of 50 kips (222 kN) was applied and maintained while instrumentation measurements were verified.

A predefined common loading protocol was used for all of the tests performed. Load was initially applied until flexural cracking was observed or a resistance of 100 kips (445 kN) was achieved. Loading was then continued in increments of 50 kips (222 kN) until critical damage and/or indications of response softening were observed. After reaching this point, loading continued until failure of the slab-column connection occurred.

Crack development and crack width growth was monitored on the tension face of each slab. Crack propagation was documented on the slab using permanent markers and the growth of the crack widths was measured using crack width comparators. Crack width monitoring was done at each load stage and documented with respect to the load measured by the data acquisition system.

Chapter. 4 Test Results

This chapter presents test observations and results. Test observations are presented in Section 4.1. Section 4.2 highlights key data obtained. Finally, Section 4.3 summarizes the main results observed over the course of the testing program.

4.1 TEST OBSERVATIONS

The test observations described herein were primarily based on the developed cracking pattern, measured crack widths, and surface damage attributed to punching cone development.

As defined in Section 3.4, a common loading protocol was used for each slab-column connection, which consisted of incrementally loading the specimens using a series of pre-defined load stages. At each load stage, testing was paused and the slabs were inspected for damage and crack development. When a critical level of damage and/or response softening was observed, the slab-column was loaded to failure.

The initial cracking patterns observed for the slabs consisted mostly of hairline cracks oriented radially and circumferentially, with approximate widths of 0.006 in. (0.15 mm). Under increased loads, substantial crack extension and new crack development were observed for all the slabs. Radial and circumferential cracks with widths of 0.010 in. (0.25 mm) were typically observed. Prior to failure, crack propagation continued and considerable crack width growth was measured for all the slab-column connections. Maximum crack widths of 0.016 in. (0.40 mm) for Slab 4 and 0.027 in. (0.70 mm) for Slab 2 were observed comprising circumferential cracks surrounding the columns of all specimens.

At the onset of failure, the regions of the slab surrounding the column were noted to have many circumferentially- and radially-oriented cracks. Radial crack widths of

0.020 in. (0.50 mm) for Slab 4 to 0.039 in. (1.00 mm) for Slab 2 were measured. Punching cones surrounding the intersecting columns were observed for all slabs (see Figure 4.1 (a) to (d)). For Slab 4 however, which did not contain shear reinforcement, the load dropped significantly in an abrupt manner immediately after failure occurred. The circumferential failure cone of Slab 4 was not as well-defined as in other slabs as the testing of the unreinforced slab was immediately terminated after the initial failure (refer to Figure 4.1 (d)). It should also be noted that the shear-reinforced connections developed considerably lower radial and circumferential crack width growth compared to that measured in the control slab at common load levels.

Additional photos presenting the propagation of damage over the course of testing are provided in Appendix. C.

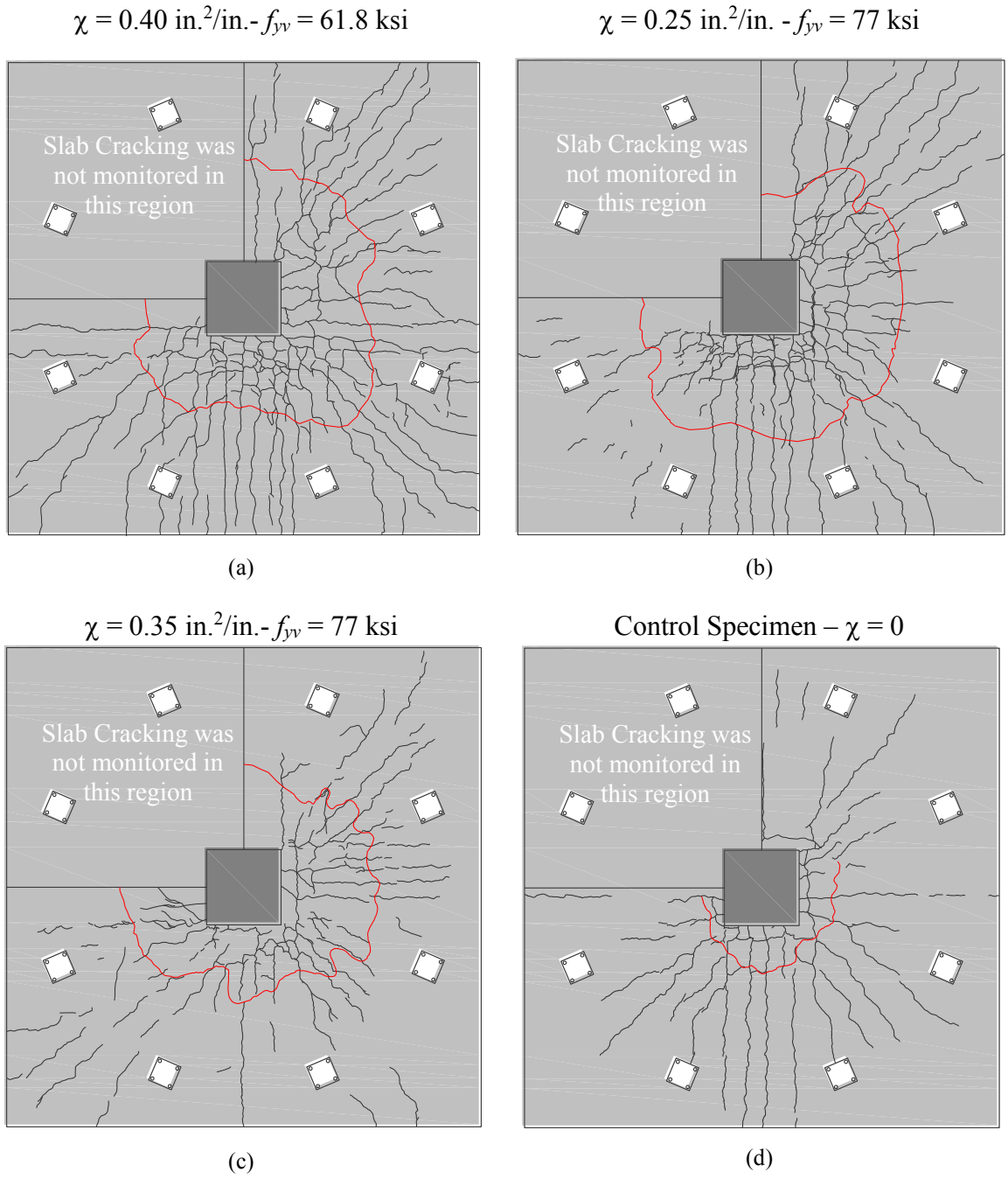

Figure 4.1: Observed Cracking Patterns at Failure; (a) Slab 1, (b) Slab 2, (c) Slab 3, (d) Slab 4

4.2 MEASURED SLAB RESPONSE

This section provides a summary of the test results obtained from the experimental program. Key results in the form of measured load-deformation and measured load-rotation responses are presented. The performance of the slab-column connections is evaluated by way of comparing the behaviors of the three shear-reinforced specimens amongst each other and in light of the performance exhibited by the slab-column connection constructed without any form of through-thickness shear reinforcement.

The normalized load-average center point displacement curves from each test are plotted and compared in Figure 4.2. The center point displacement (Δ_{mid}) was taken as the average of the relative displacement measurements obtained as the difference between the vertical displacement pertaining to the support strut reaction locations and the measured vertical displacements of the slabs immediately adjacent to the column. From Figure 4.2, it can be observed that regardless of shear reinforcement system employed, the shear-reinforced specimens exhibited similar initial stiffness characteristics. Stiffnesses of the four slabs were nearly identical prior to the formation of the flexural cracking (i.e., at load levels of less than approximately 100 kips (450 kN)). However, after some degree of flexural cracking had occurred, the post-cracking stiffness was found to vary marginally amongst the specimens. Slab 1 had the highest post-cracking stiffness, while the stiffness for Slabs 2 and 3 were found to be similar.

The large differences amongst the capacities of the four slabs are summarized in Table 4.1. Slab 4 had the lowest capacity due to the fact that it was constructed without any through-thickness reinforcement. As a result, the measured slab displacement and slab rotation values at the failure load were approximately 30 % to 50 % less than those measured for the shear reinforced specimens. Although slabs 1 and 2 were designed,

according to the provisions of ACI 318-14, to develop equal shear resistances, the maximum loads obtained for these slabs differed greatly, as shown in Figure 4.2 and Table 4.1. The resistances obtained for the specimens containing inclined shear reinforcement (Slabs 2 and 3) were much lower than that obtained for the slab reinforced with vertically-oriented shear reinforcement (Slab 1). It should also be noted that although Slab 3 was reinforced such that a greater shear reinforcement ratio was provided at the critical section, the capacity obtained for Slab 2 was only marginally less than that achieved by Slab 3.

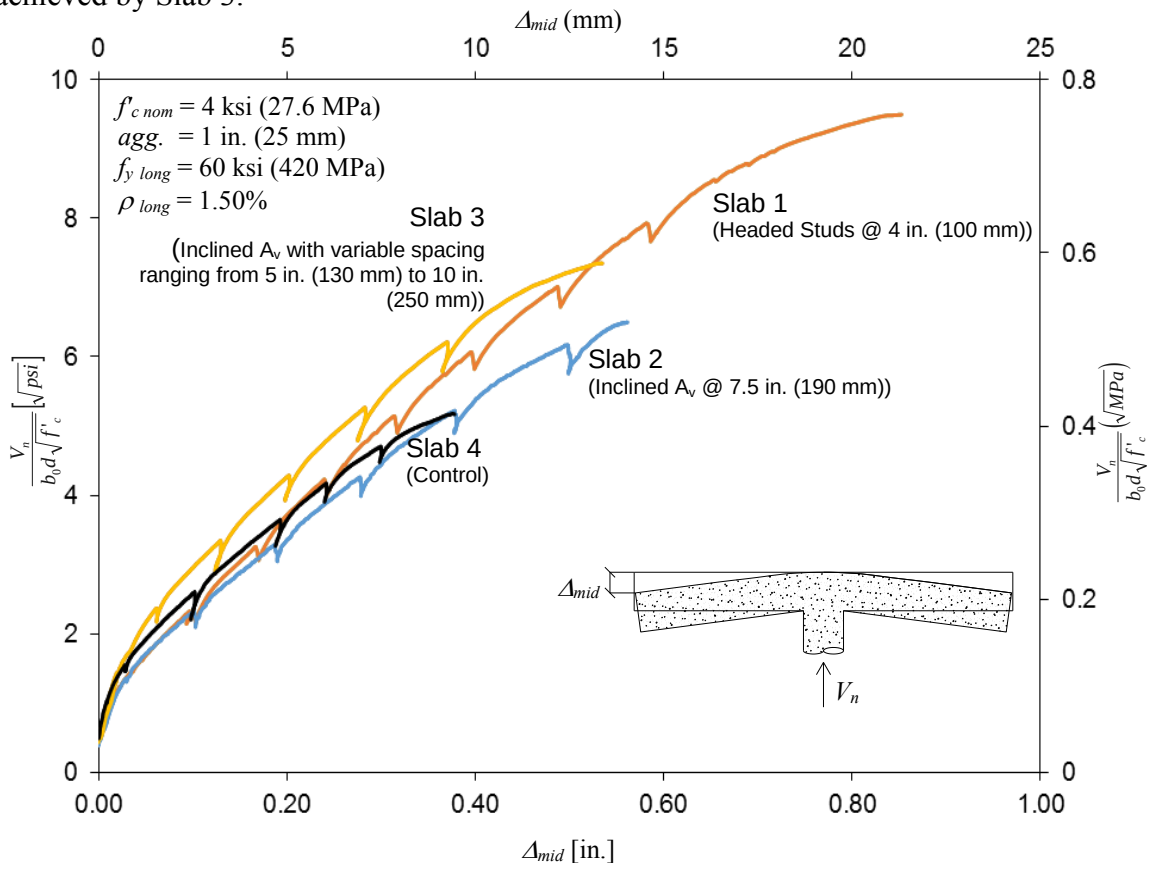

Figure 4.2: Normalized Shear Force-Center Point Displacement

From the test data summarized in Table 4.1, it can be seen that the four slabs comprising the experimental program exhibited similar responses up to the point of initial

shear crack development. The initial cracking load for each specimen was estimated graphically on the basis of the load level at which the load-shear reinforcement strain response showed a deviation from the initial near-linear response. It was determined that the loads causing shear crack development throughout the critical region was virtually the same for all the slab-column connections.

Table 4.1: Summary of observed responses

Load Stage	Parameter	Slab 1	Slab 2	Slab 3	Slab 4
Initial Shear Cracking	Load [kips (kN)]	250 (1112)	250 (1112)	275 (1123)	246 (1094)
At Failure	Maximum Load [kips (kN)]	511 (2273)	350 (1557)	382 (1699)	246 (1094)
	Center Point Displacement [in. (mm)]	0.85 (23)	0.56 (14)	0.53 (14)	0.37 (9.6)
	Average Rotation [rad.]	0.0173	0.0114	0.0108	0.0076

4.3 SUMMARY

An experimental testing program comprised of four full-scale RC slab-column connections subjected to punching shear loading conditions was performed. From the observations made over the course of the testing program, the following was found:

- All specimens experienced near-identical response in terms of crack development and patterns. However at a common load level of 246 kips (1094 kN) (i.e., failure load level of Slab 4), smaller width cracks were observed to occur in the slabs containing shear reinforcement in comparison to those developed in the slab without any form of shear reinforcement (i.e., Slab 4, control specimen).

- With respect to measured load-deformation, at moderate and near-failure load levels, the specimens constructed with shear reinforcement achieved greater slab displacements and rotations than the slab constructed without shear reinforcement.
- The shear capacities of the slabs varied greatly as a result of the shear reinforcement provided. The capacity of Slab 1 (reinforced with vertically-oriented through thickness reinforcement) was significantly greater than that obtained for all other slabs. Slabs 2 and 3 (possessing inclined shear reinforcing members) failed at similar load levels, and Slab 4, which was constructed without shear reinforcement, had the lowest capacity. However, the applied load that produced the initial development of the critical shear crack was estimated to be similar for all slabs.
- In all cases, the governing failure mode was controlled by slab punching. Failure occurred in a highly brittle manner, without warning and with only limited indications of the ensuing failure.

Chapter. 5 Analysis and Discussion

This chapter presents in-depth discussion and examination of the results obtained from the experimental program. Section 5.1 presents a series of supplementary analyses conducted to better understand the merits and limitations of flat slabs constructed with the novel inclined shear reinforcement system. This chapter also highlights the suitability of several codes of practice in estimating the punching shear strength of RC flat slabs. Section 5.2 investigates the two-way shear design capacity according to various provisions, while Section 5.3 provides a discussion regarding the influences of the premature anchorage failures observed and the consideration of this mechanism within codified procedures. Lastly, Section 5.4 presents key findings obtained from the analysis and discussion herein.

5.1 ANALYSIS OF TEST RESULTS

5.1.1 Load Carried by Shear Reinforcement

Figure 5.1 (a) presents measured strain data pertaining to the slab constructed with the headed stud rail assemblies (Slab 1), and Figure 5.1 (b) presents the strain measurements for the slab constructed with the equally-spaced inclined shear reinforcement system (Slab 2). Note that all of the strain gages used to develop the relationships presented in Figure 5.1 were installed at the mid-height location of the shear reinforcement working members.

From Figure 5.1 (a), it is evident that the headed studs comprising the most critical regions developed strains indicative of stud yielding. In contrast, the curves shown in Figure 5.1 (b) reveal that only limited strain levels were developed at the mid-depth of the inclined working members with no evidence of yielding. Thus, in the case of

Slab 2, it is apparent that the full strength of the reinforcing working members was not reached. Data obtained for Slab 3 indicated similar strain response as Slab 2 with limited working member strain development prior to failure and no yielding.

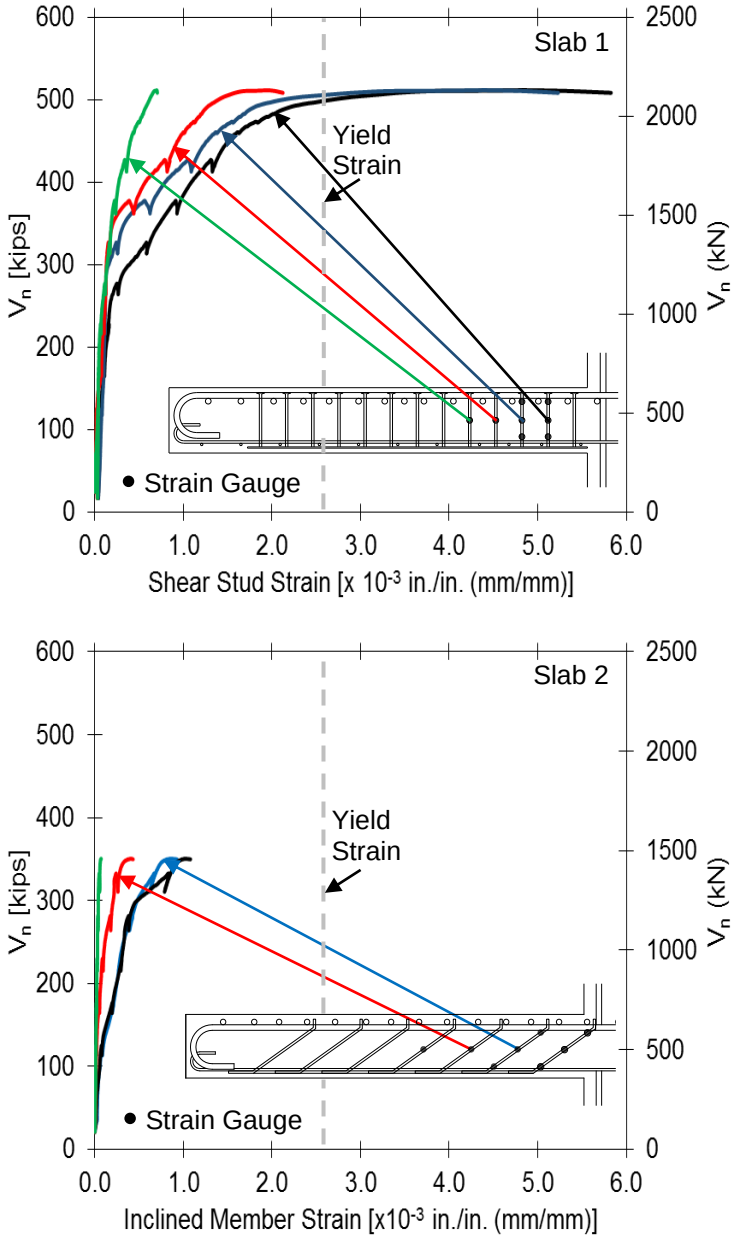

Figure 5.1: Load-Mid-Depth Shear Reinforcement Strain Response

5.1.2 Flexural Response

The slabs were designed to ensure that yielding of the flexural reinforcement did not occur prior to the slab failing in shear. The normalized load-tensile longitudinal reinforcement strain curves presented in Figure 5.2 confirm that the flexural reinforcement remained in the linear-elastic range for the duration of the tests. It can be observed that all of the tests resulted in a failure at similar strain levels, prior to reaching approximate yield strain.

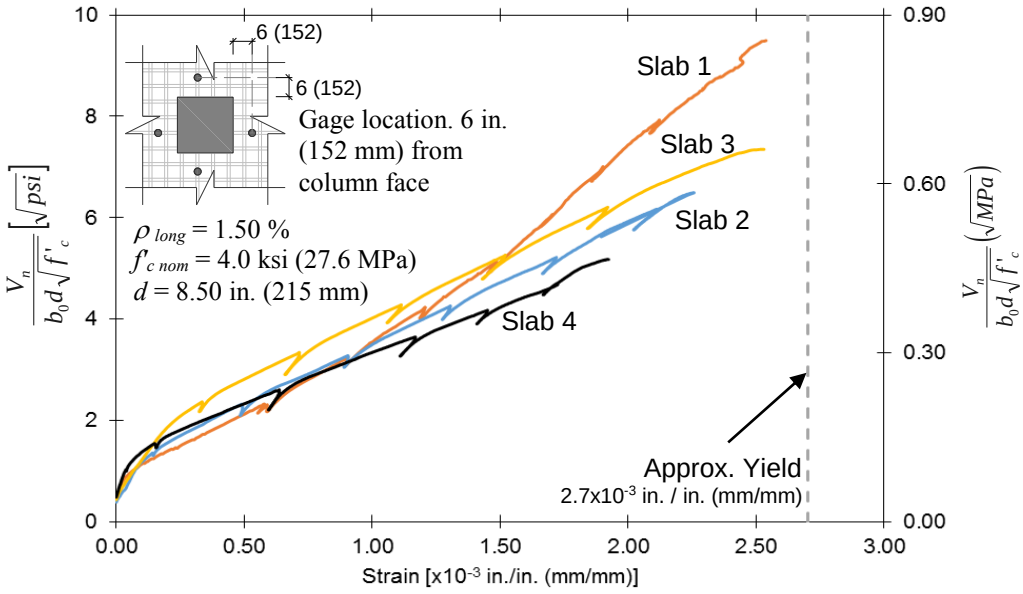

Figure 5.2: Normalized Load-Tensile Longitudinal Strain

5.1.2.1 Influence of Bending on Inclined Reinforcement

Bending deformations were shown to play a significant role on the strains developed in the inclined members serving as the shear reinforcement in Slabs 2 and 3. Note that the distance from the flexural tensile reinforcement to the strain gages placed at the top of the working members varied amongst the East-West and North-South

directions. The East-West direction of the slabs had a greater effective depth ($d_{E\text{-}W}$ = 8-3/4 in. (220 mm)) and hence, a greater flexural stiffness than that of the North-South direction ($d_{N\text{-}S}$ = 8-0 in. (200 mm)). Thus, the longitudinal reinforcement placed along the East-West direction constituted the strong-axes of bending while the longitudinal reinforcement placed along the North-South direction constituted the weak-axes of bending. Another important difference amongst Slabs 2 and 3 is the longitudinal distance from the face of the column to the top hook of the inclined working member, which was 5-13/16 in. (147 mm) for Slab 2 and 3-5/16 in. (84 mm) for Slab 3.

Figure 5.3 presents the strain measurements obtained at different locations along the height of the working members positioned within the critical region. The lack of variation amongst the strains measured over the height of the headed smooth stud is indicative of the negligible bond provided by the smooth bars (refer to Figure 5.3 (a)). From Figure 5.3 (b), it can be observed that the strain measurements from the gages located at the middle and bottom portions of the inclined reinforcing member were similar. However, the strain gage located at the top of the working member showed considerably larger strains shortly after flexural cracking occurred. The strain development measured for Slab 3 was similar to that obtained for Slab 2. Therefore, it can be assumed that bending affected the strain variation in Slab 2 and Slab 3.

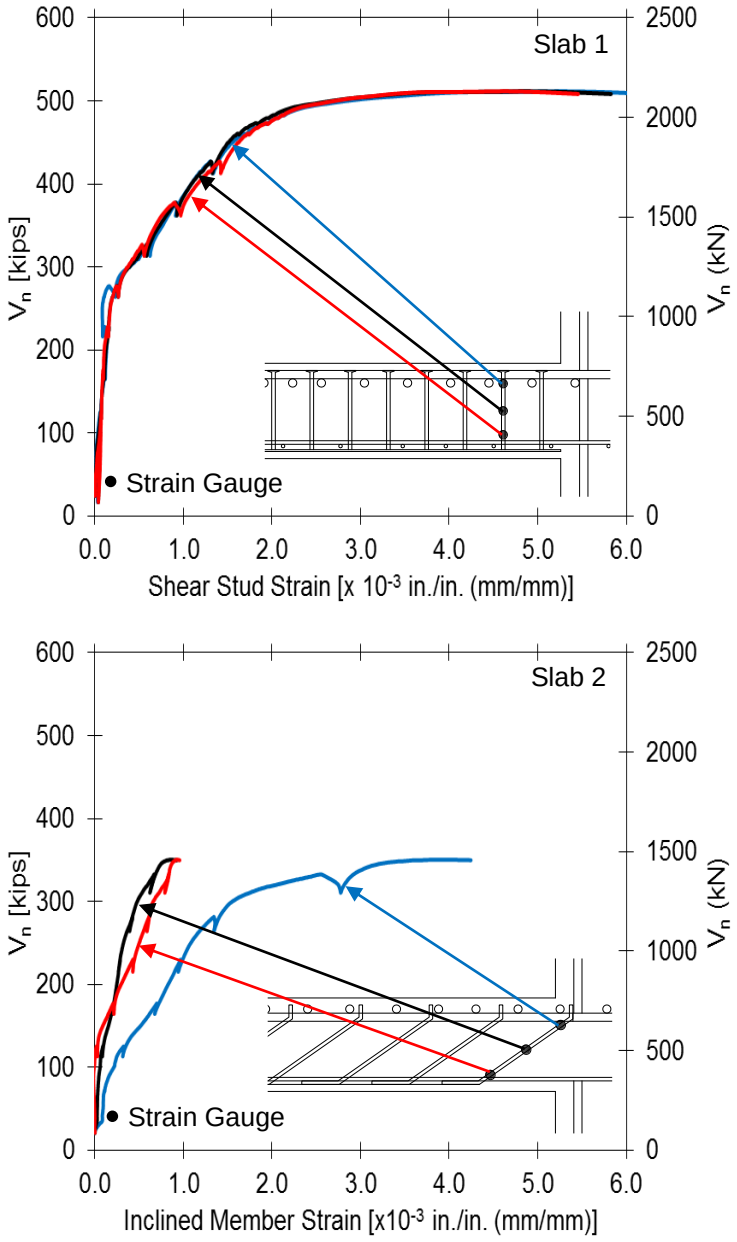

Figure 5.3: Measured Strain Variation over the Height of the Shear Reinforcement Working Members

5.1.3 Damage and Controlling Failure Modes

Over the course of testing, circumferential shear crack development was observed in all slabs. To examine the internal cracking, the slabs were saw-cut after testing and the damage was documented, as shown in Figure 5.4. From the figure, it can be estimated that three headed studs per assembly were effectively engaged by the critical shear crack(s) developed in Slab 1. In Slabs 2 and 3, it can be observed that only two inclined members per assembly were effectively engaged by the critical shear crack(s). Although Slabs 1 and 2 were designed with equal V_s as per ACI 318-14, the smeared approach used in the procedure did not adequately capture the critical influence of working member-shear crack engagement.

Figure 5.4: Cross Section of the Failure Modes (partial cross section shown); (a) Slab 1, (b) Slab 2, (c) Slab 3, (d) Slab 4

It is critical that shear reinforcement be adequately anchored and hence, be capable of developing its full yield capacity. All analyzed code provisions explicitly

mention in their associated detailing provisions that well anchored stirrups must enclose the longitudinal reinforcement in the punching zone to ensure adequate anchorage. For headed stud rails, the anchorage is provided by way of mechanical anchor heads and welded steel rails. As such, for Slab 1, the specimen was able to transfer forces across the critical shear cracks long after the headed studs developed their yield strengths. However, for Slabs 2 and 3, it was found that the hooked end-anchors provided at the tops of the inclined working members, in combination with the anchorage developed as a result of reinforcing bar deformations, were not sufficient in allowing the inclined working members to fully develop their yield capacities and, therefore, the inclined members were not fully utilized.

5.1.4 Anchorage Requirements

The hooked end-anchors provided for the free-ends (i.e., the end regions located on the tension side of the slab) of the inclined working members serving as the shear reinforcement in Slabs 2 and 3 were found to be insufficient. Strains measured in the shear reinforcement indicated that the hooked-end anchors did not prevent slip/pull-out from occurring (see Figure 5.5). It should also be noted that the hooked-end anchors are located in regions of the slabs that experience high longitudinal tensile strains due to flexure, and therefore, must provide adequate anchorage in concrete regions that develop extensive vertical cracking. Thus, the pull-out failures that occurred were attributed to steel-concrete bond degradation in extensively cracked concrete.

(a)

(b)

Figure 5.5: Anchorage Pull-Out Failure; (a) Slab 2, (b) Slab 3

5.2 SUITABILITY OF CODE PROVISIONS

To establish the two-way shear design capacity of the RC slab-column connections, the provisions of ACI 318-14, *fib* Model Code 2010, Eurocode 2, and the CSCT behavioral model were considered. Note that, for comparative purposes, nominal values for the cylindrical compressive strength of concrete and the yield strength of steel were used (f'_c = 4.0 ksi (27.6 MPa), f_y = 60 ksi (420 MPa), f_v = as provided, ρ_l = 1.50 %).

Table 5.1 presents a summary of the punching shear strengths computed using the aforementioned code provisions for each slab-column connection comprising the testing

program. Figure 5.6 summarizes the estimated resistances provided by the shear reinforcement for each of the specimens constructed with out-of-plane reinforcement.

Table 5.1: Summary of Estimated Two-Way Shear Strengths (f'_c = 4.0 ksi (27.6 MPa), f_v = as provided, ρ_l = 1.50 %)

	Slab 1 f_v = 63.1 ksi (435 MPa)			Slab 2 f_v = 77.8 ksi (536 MPa)			Slab 3 f_v = 77.8 ksi (536 MPa)			Slab 4		
	V [kips (kN)]	V_c [kips (kN)]	V_S [kips (kN)]	V [kips (kN)]	V_c [kips (kN)]	V_S [kips (kN)]	V [kips (kN)]	V_c [kips (kN)]	V_S [kips (kN)]	V [kips (kN)]	V_c [kips (kN)]	V_S [kips (kN)]
ACI (2014)	373 (1657)	158 (703)	215 (954)	316 (1406)	105 (469)	216 (961)	316 (1406)	105 (469)	324 (1442)	211 (937)	211 (937)	0 (0)
fib (2010)	340 (1514)	170 (757)	202 (898)	285 (1268)	212 (943)	73 (326)	285 (1268)	212 (943)	73 (326)	239 (1065)	239 (1065)	0 (0)
EC 2 (2004)	402 (1789)	177 (789)	225 (1000)	253 (1126)	177 (789)	76 (337)	291 (1294)	177 (789)	113 (505)	237 (1052)	237 (1052)	0 (0)
CSCT (2009)	415 (1845)	231 (1026)	184 (819)	368 (1636)	252 (1121)	116 (515)	374 (1663)	249 (1108)	125 (555)	292 (1299)	292 (1299)	0 (0)

Note: Level of approximation 2 was used for *fib* calculations (see Appendix. A)

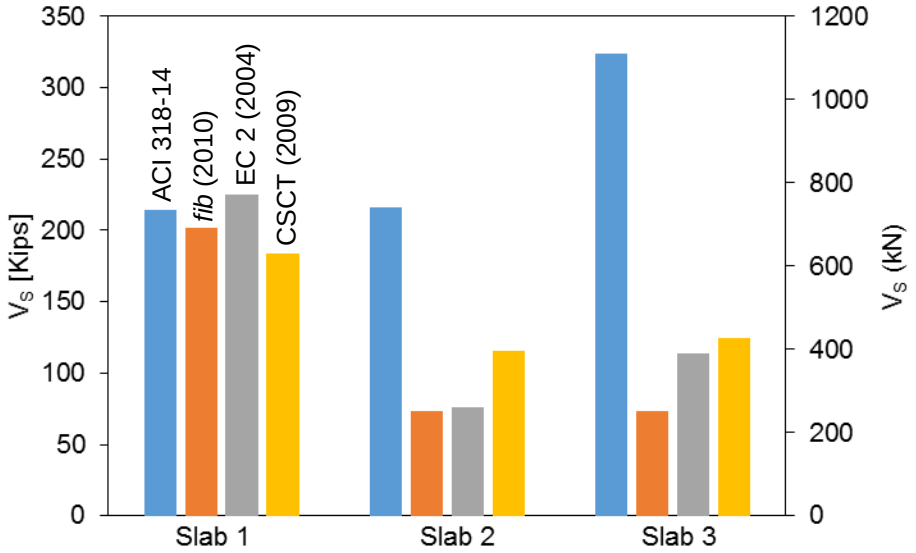

Figure 5.6: Estimated Shear Resistance Provided by Shear Reinforcement, V_s

Figure 5.6 shows that the largest estimated resistance values provided by the shear reinforcement were obtained using the ACI 318-14 procedures for Slabs 2 and 3; however, the application of the Eurocode 2 (EC2) provisions led to the largest shear reinforcement strength for Slab 1. This difference is attributed to the fact that EC2 applies a factor of 1.50 to the resistance provided by shear reinforcement. The larger values of shear strength reached by both ACI 318-14 and Eurocode 2 relative to those obtained from the other studied provisions can be explained by the fact that neither provision considers a discrete computation of the number of shear reinforcing members that cross the shear crack (i.e., it is possible to have partial working members (e.g., 2.5 studs) crossing a crack). In addition, the formulations provided by ACI 318-14 do not account for the influence of longitudinal reinforcement ratio nor the size effect, while the Eurocode 2 considers both effects (refer to Appendix. A).

CSCT estimates the largest values of shear strength in comparison to those provided by the other provisions. Additionally, while CSCT serves as basis for the *fib* Model Code 2010, there is a difference in the values of the total shear capacity computed from the two procedures. As illustrated in Muttoni et al. (2013), since *fib* Model Code 2010 was developed to serve as code-suitable formulation, there are certain simplifications that were made to ease the calculation procedure (i.e., k_{ψ}), and, as a result, in many cases, the *fib* provisions led to smaller values of punching shear capacity than those obtained from the CSCT, for this test series.

Lastly, the ACI 318-14 and the *fib* Model Code 2010 calculations suggest that slab failures are controlled by crushing of the concrete (refer to V obtained in Slab 3 for ACI 318-14, and Slab 1 for *fib* 2010 in Table 5.1). In these provisions, the crushing of the concrete strut is determined from the compressive concrete strength, geometrical parameters of the specimens, and constants obtained from experimental results. There is

no direct relationship between this mode of failure and the mechanical behavior of the slab when subjected to punching shear loading conditions. However, CSCT also includes the rotation of the slab, and takes into account size effect for determining this mode of failure (size effect is also considered in the Eurocode 2 procedures). Therefore, it is expected to obtain larger values for strut crushing capacity as it explicitly accounts for the influences of flexural deformations on slab capacity and does not employ the same broad-spanning simplifying assumptions used in the design procedures.

5.3 ACCOUNTING FOR PREMATURE FAILURE

This section is intended to establish the validities of the slab-column capacity estimates provided by the provisions of ACI 318-14, *fib* Model Code 2010, Eurocode 2, and the CSCT behavioral model, considering actual material properties (i.e., f'_c) and the influence of shear reinforcement anchorage. The results from the provisions are compared to those observed from the experimental program.

Amongst all of the provisions considered, only the CSCT and the *fib* Model Code 2010 consider the bond stress capabilities of the shear reinforcing bars when calculating the punching capacity of shear-reinforced slabs. A meaningful approach to study the likelihood of a premature anchorage failure occurring is by analyzing the bond strength of such elements. Therefore, a variety of scenarios have been considered in the calculations performed using the CSCT and *fib* Model Code 2010:

(a) In the work conducted by Fernandez Ruiz and Muttoni (2009), it was suggested that the bond strength (τ_{bd}) be taken equal to 0.44 ksi (3.0 MPa) when bond is considered to be activated on both sides of a critical shear crack and a rigid perfectly-plastic bond law is assumed.

(b) According to the procedures of the *fib* Model Code 2010, reinforcement bond strength can be estimated as:

$$f_{bd} = (\alpha_2 + \alpha_3) f_{bd,0} - 2\frac{p_{tr}}{\gamma_c} < 2.5 f_{bd,0} - 0.4\frac{p_{tr}}{\gamma_c} < 1.5\frac{\sqrt{f_{ck}}}{\gamma_c} \qquad (5\text{-}1)$$

where f_{bd} is the design bond strength. (5-1) accounts for the influence of passive confinement from cover as well as from transverse reinforcement (i.e., α_2 and α_3, respectively), and for the stress perpendicular to the potential splitting failure at ultimate (i.e., p_{tr}). (5-1) is also dependent on what is called the basic bond strength:

$$f_{bd,0} = \eta_1\eta_2\eta_3\eta_4\left(\frac{f_{ck}}{25}\right)^{\frac{0.5}{\gamma_c}} \qquad (5\text{-}2)$$

where η_1 to η_4 are parameters that reflect the geometry of the bars (i.e., ribbed or smooth), position of the reinforcement at the time of casting, diameter of the reinforcing bars, and the characteristic strength of the steel, respectively. Using (5-1) and (5-2), an allowable bond strength estimate of 0.27 ksi (1.86 MPa) was estimated for Slabs 2 and 3.

(c) Considering that large width cracks and appreciable damage were observed on the flexural tension sides of the slabs, the presence of longitudinal tensile stresses in concrete between the cracks, and hence, the post-cracking tensile response of the concrete was taken into account to estimate tensile stress related degradation. The tension stiffening formulation provided by Collins and Mitchell (1997) was considered:

$$f_c = \frac{f_{cr}}{1 + \sqrt{500\varepsilon_{cf}}} \qquad (5\text{-}3)$$

where f_c represents an average tensile stress in the cracked reinforced concrete, f_{cr} is the cracking stress of the concrete (taken as $2.0\sqrt{f_c'}$ in units of psi ($0.33\sqrt{f_c'}$ in units of MPa)), and ε_{cf} is the average tensile strain developed at the location of the tensile

mat of reinforcement. Average tensile stress estimates were then used to determine the bond strength according to the *fib* Model Code 2010 procedures mentioned in (b). In this case, a reduced bond strength value of 0.18 ksi (1.25 MPa) was obtained.

Note that the prefabricated shear stud rail assemblies used in the testing program are designed to independently develop required end anchorage. As such, no consideration of the bond stress development between the headed studs and the surrounding concrete was taken into account as the studs comprising the shear stud reinforcement assembly were anchored to the concrete by way of mechanical heads and welded steel rails, and were shown to yield. Therefore, Slab 1 has been omitted from these analyses.

Table 5.2 summarizes the punching shear capacity estimated by the different provisions and the measured results obtained from the testing program. The table includes information pertaining to the shear capacity, the stresses developed in the shear reinforcement, and the rotations of the slabs at ultimate. Additionally, Figure 5.7 illustrates the resistance provided by the shear reinforcement for each shear-reinforced slab-column connection.

Note that the computed stress activated in the shear reinforcement depends mainly on the bond stress development. Lower values of the activated stresses are estimated when bond strength values are determined by the application of the tension stiffening model. The lowest working stresses were computed from the application of the *fib* Model Code 2010 and the Eurocode 2 procedures (~50 % to 60 % of the yield stress), whereas the ACI 318-14 estimated full yield for all the specimens.

The estimated values of slab rotation at failure illustrate the slab dependence on the code procedure used. The largest shear strength estimates from all of the shear-reinforced slab configurations were computed using the CSCT behavioral model. In contrast, and due to its code-like nature, the *fib* Model Code 2010 procedures provided

rather conservative strength values in comparison to those measured from the testing program (i.e., ~70 % of the actual rotation at failure). Both ACI 318-14 and EC 2 provisions do not consider the slab rotation for the estimation of the punching shear capacity.

Table 5.2: Summary of Punching Shear Failure Criterion. Actual Values

	τ_{bd}	Slab 2 f'_c = 4194 psi (28.9 MPa), f_y = 73.5 ksi (507 MPa), f_v = 77 ksi (531 MPa)					Slab 3 f'_c = 3906 psi (26.9 MPa), f_y = 73.5 ksi (507 MPa), f_v = 77 ksi (531 MPa)				
		ψ	σ	V	V_c	V_S	ψ	σ	V	V_c	V_S
	[ksi (MPa)]	[rad]	[ksi (MPa)]	[kips (kN)]	[kips (kN)]	[kips (kN)]	[rad]	[ksi (MPa)]	[kips (kN)]	[kips (kN)]	[kips (kN)]
ACI (2014)	-	-	77 (531) 100%	322 (1432)	108 (480)	214 (952)	-	77 (531) 100%	312 (1389)	104 (463)	321 (1428)
fib (2010)	0.44 (3.00)	0.00956	46 (315) 59%	286 (1271)	193 (861)	92 (411)	0.00942	45 (310) 58%	279 (1242)	188 (837)	91 (404)
	0.27 (1.86)	0.00928	41 (285) 54%	280 (1246)	197 (875)	83 (371)	0.00914	41 (281) 53%	274 (1217)	191 (851)	82 (366)
	0.18 (1.25)	0.00913	39 (268) 51%	277 (1232)	198 (883)	79 (350)	0.00899	38 (264) 50%	271 (1203)	193 (859)	77 (344)
EC 2 (2004)	-	-	44 (304) 57%	245 (1091)	170 (755)	76 (337)	-	44 (304) 57%	279 (1242)	166 (737)	113 (505)
CSCT (2009)	0.44 (3.00)	0.01369	75 (515) 97%	363 (1614)	234 (1043)	128 (571)	0.01392	75 (519) 98%	362 (1611)	224 (998)	138 (613)
	0.27 (1.86)	0.01254	57 (390) 73%	342 (1523)	245 (1090)	97 (433)	0.01264	57 (392) 74%	340 (1510)	236 (1048)	104 (462)
	0.18 (1.24)	0.0118	38 (261) 49%	329 (1463)	252 (1123)	76 (340)	0.01182	40 (278) 52%	325 (1444)	243 (1083)	81 (362)
Tests	-	**0.01140**	- -	**350 (1557)**	-	-	**0.01080**	- -	**382 (1699)**	-	-

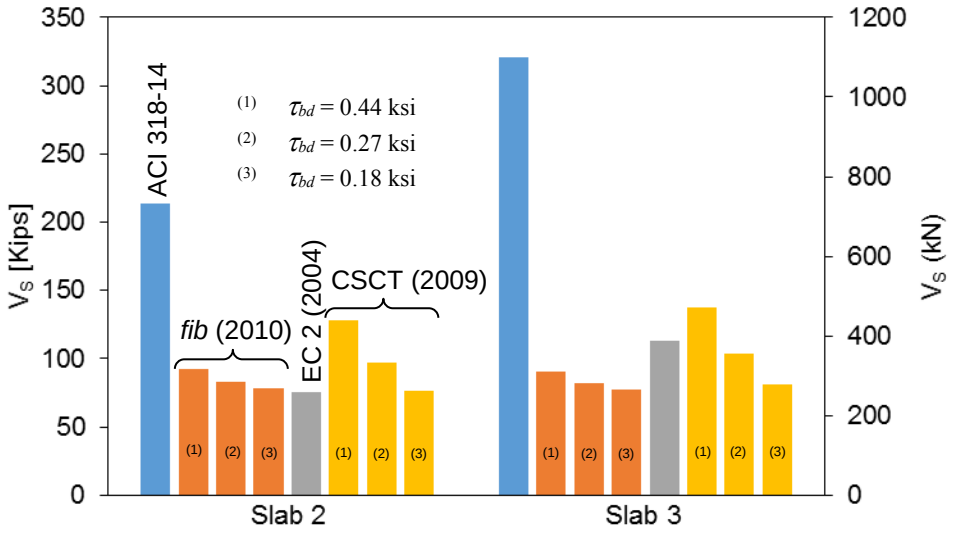

Figure 5.7: Estimated Shear Resistance Provided by Shear Reinforcement. Actual Values

Table 5.3 provides a comparison of the punching shear strengths measured from the experimental program to those estimated using the code provisions (note that values over 1.0 reflect conservative estimations). Also note that the tested-to-calculated values were not computed for Slab 1 using the CSCT and *fib* provisions as they are based on the bond strength and do not consider mechanical anchorage provided by the shear studs.

Table 5.3: Comparison of Code Provisions to Test Results

	V_{test} / V_{prov}							
	ACI	*fib*			EC 2	CSCT		
τ_{bd}[ksi]	-	0.44	0.27	0.18	-	0.44	0.27	0.18
Slab 1	1.38	-	-	-	1.29	-	-	-
Slab 2	1.09	1.23	1.25	1.26	1.43	0.96	1.02	1.06
Slab 3	1.22	1.37	1.40	1.41	1.37	1.05	1.13	1.18
Slab 4	1.29	1.21	1.21	1.21	1.21	1.21	1.21	1.21
Average	1.24	1.27	1.29	1.30	1.32	1.08	1.12	1.15
COV	0.085	0.056	0.062	0.066	0.062	0.094	0.069	0.054

The results obtained from the ACI 318-14 and the Eurocode 2 procedures are rather conservative, which is to be expected from design oriented provisions. Yet, both codes of practice provided consistent conservatism on the basis of the low computed variations.

For the CSCT behavioral model, a satisfactory agreement is found between the measured punching shear strength in the tested specimens and the calculated punching shear strength, with an average experimental-to-computed strength ratio of 1.10 and coefficient of variation (COV) of 7 %. Similar COVs are also found for the *fib* Model Code 2010 predictions. However, an average experimental-to-computed strength estimate ratio of 1.28 was obtained using the *fib* Model Code 2010, illustrating more-conservative estimates.

Note that the application of different values of bond strength to both CSCT and *fib* Model Code 2010 procedures did not significantly modify the shear capacity of the shear-reinforced flat slabs. The difference between the values of shear strength following a rigid perfectly-plastic bond law and those following a tension stiffening approach is of about 10% for the CSCT and around 3% for the *fib* Model Code 2010 (see Table 5.2 and Table 5.3). However, as shown in Table 5.4, the estimations for Slabs 2 and 3 using a bond strength value of 0.27 ksi (1.86 MPa) have shown an approximate increase of more than 30 % of the shear reinforcement ratio would be needed to achieve the same punching capacity as that obtained considering a rigid perfectly-plastic bond law. The amount of shear reinforcement would be further increased if a 0.18 ksi (1.25 MPa) bond strength value was used, as shown in Table 5.4, with an increase of more than 80 % of shear reinforcement being required.

Table 5.4: Required Shear Reinforcement Ratio Considering Bond Stress Development

τ_{bd} [ksi (MPa)]	Slab 2 ρ_v [%]	Slab 3 ρ_v [%]
0.44 (3.00)	0.34	0.51
0.27 (1.86)	0.46	0.67
0.18 (1.25)	0.61	0.92

Note: Calculations performed using CSCT

5.4 SUMMARY OF DISCUSSION

The analysis and discussion presented in this chapter can be summarized by the following key findings:

- Bending deformations were found to influence the strain development and associated stresses for the inclined shear reinforcement assemblies. Thus, the inclined nature of the working members effectively reduced the working member stress capacity available to resist shear.
- Slab failures occurred in a highly brittle manner. For the shear-reinforced slabs, these failures occurred after critical shear crack formation and, as a result, significantly greater damage was developed.
- The slabs containing the inclined shear reinforcement system were controlled by premature anchorage failures. The inclined working members were unable to develop their yield capacities. The anchorage failure occurred as a result of hooked end-anchor pull-out. Additionally, the punching shear capabilities for these specimens were significantly less than the strength developed by the slab reinforced with comparable ratios of vertically oriented shear studs.

- All codes of practice were found to be conservative when compared to the results obtained from the experimental program. However, the values given by following the CSCT behavioral model were most-correlated with the experimental results, correctly describing both the strength and the deformation at failure.
- Examination of the codes of practice revealed that there is no direct and simple approach to account for premature anchorage-induced failures within the existing design provisions. However, ACI 318-14, Eurocode 2, and *fib* Model Code 2010 do provide a series of detailing provisions aimed toward preventing or mitigating the onset of premature failures principally attributed to poor anchorage conditions.

Chapter. 6 Conclusions

Several conclusions regarding the performance of RC flat slabs constructed with the novel inclined shear reinforcement system can be made. For clarity, findings from the testing campaign and the analytical studies are presented separately.

With respect to the experimental program, the following conclusions can be drawn:

- Considerable stress development in the inclined working members comprising the novel shear reinforcement system due to flexural deformations in the slab surrounding the column connection area was observed. The strains measured in the inclined reinforcing elements were engaged at low applied shear force levels (around 20 % to 30 % of failure load).
- At low and moderate load levels (~ 50 % of V_n), improvements in terms of shear crack distribution and crack width control were observed for the slabs containing the novel shear reinforcement system relative to those constructed with vertically-oriented through-thickness studs. It was also observed that all shear-reinforced specimens experienced brittle failure modes following the formation of the critical shear crack.
- Limited strain levels were developed in the inclined working members even though flexural deformations were shown to engage the inclined working members.
- The test results have shown that the hooked end-anchors of the inclined working members were not adequate in preventing slip/pullout from occurring and, as a result, were unable to develop their yield capacities prior to failure. As the hooked end-anchors are located in the flexural tensile regions of the RC slabs, vertical

cracking was also developed. As such, the pull-out failures observed in Slabs 2 and 3 were attributed to bond degradation in extensively cracked concrete.

To assess the suitability of codes of practice when estimating the punching shear capacity of RC flat slabs, a study of several provisions was conducted. The following was found:

- All studied code provisions were shown to provide conservative shear strength estimates for the tested slabs. However, the CSCT behavioral model was found to correlate best with test results. This can be explained by the fact that this theoretical model explicitly accounts for size and strain effects by means of mechanical and geometrical parameters.
- Both ACI 318-14 and Eurocode 2 do not take into account bond strength of shear reinforcement in their calculations. However, while ACI 318-14 considers full yield of the shear working members to estimate the resistance provided by shear reinforcement, Eurocode 2 determines the working stress level of steel as a function of the slab thickness.
- It has been shown that shear resisting mechanisms of RC members depend on bond stress development between the steel working members and the surrounding concrete; however, only *fib* Model Code 2010 and CSCT consider the bond strength as an input parameter to estimate the punching shear capacity of RC flat slabs. Bond stress development along the lengths of the inclined shear reinforcing members has shown to produce little impact on the punching shear estimates. However, the amount of required shear reinforcement placed in the slab-column connections is a function of the bond stress development.
- There is no direct calculation in the studied provisions to predict premature failure attributed to poor anchorage conditions. However, all codes of practice establish a set of detailing rules that need to be followed to prevent the occurrence of such

mode of failure. In this sense, both ACI 318-14 and Eurocode 2 explicitly mention that the hooks in the tension zone of the slab must enclose the longitudinal reinforcement to ensure proper anchorage. If not, premature failure due to a pull-out effect may occur. Other research programs have also remarked the importance of having longitudinal reinforcement enclosed by shear reinforcement. Enclosing longitudinal bars by way of hooks or other configurations (i.e. welded horizontal runners) is especially important in the zone of RC members subjected to tensile stresses. Therefore, it is likely that the lack of longitudinal bars enclosed by the hooked end-anchors could have triggered the pull-out failure observed in the experimental testing program.

Appendix. A Code Background

This appendix provides an overview of several formulations used to design two-way flat slabs.

A.1 ACI 318-14 (BUILDING CODE REQUIREMENTS FOR STRUCTURAL CONCRETE)

In the design of two-way shear-reinforced slab-column connections, ACI 318-14 assumes that a fraction of the load applied to the slab is carried by concrete and some fraction is resisted by shear reinforcement:

$$V_n = V_c + V_s \tag{A-1}$$

V_c = Nominal shear strength provided by concrete.

V_s = Nominal shear strength provided by shear reinforcement.

For nonprestressed slabs, the concrete contribution is taken as the minimum of:

$$V_c = \left(2 + \frac{4}{\beta}\right)\lambda\sqrt{f'_c}\,b_o d \tag{A-2}$$

where β is the ratio of long side dimension to short side dimension of the column, concentrated load, or reaction area, and λ is a factor that accounts for the use of lightweight concrete;

$$V_c = \left(\frac{\alpha_s d}{b_o} + 2\right)\lambda\sqrt{f'_c}\,b_o d \tag{A-3}$$

where α_s is taken as 40 for interior columns, 30 for edge columns, 20 for corners columns; and

$$V_c = 4\lambda\sqrt{f'_c}\,b_o d \tag{A-4}$$

When shear reinforcement perpendicular to the longitudinal axis is used, the shear strength contribution provided by the reinforcement is taken as:

$$V_s = \frac{A_v f_{yt} d}{s} \qquad \text{(A-5)}$$

where A_v shall be taken as the cross-sectional area of all legs of reinforcement on one peripheral line that is geometrically similar to the perimeter of the column section (i.e., along perimeter b_0) (see Figure A.1).

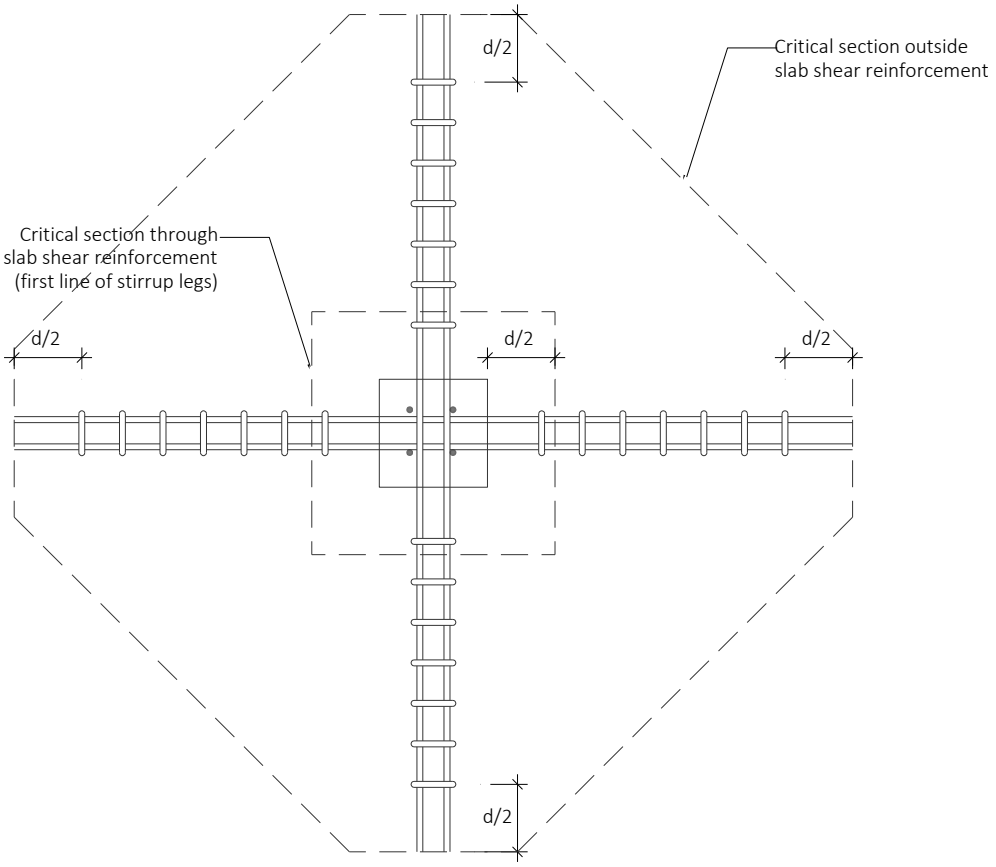

Figure A.1: Arrangement of stirrup shear reinforcement, interior column (Adapted from ACI 318-14)

When inclined stirrups are provided as shear reinforcement, their shear strength contribution is taken as:

$$V_s = \frac{A_v f_{yt}(\sin\alpha + \cos\alpha)d}{s} \qquad \text{(A-6)}$$

where α is the angle between inclined stirrups and longitudinal axis of the member. In this expression, it is implicit that the shear crack crosses an average number of more than one inclined stirrups. That is, reinforcement is treated in a smeared fashion and no check is performed to compute the number of discrete shear reinforcing members that will be crossed by a 45-degree shear crack assumed.

ACI 318-14 limits the nominal shear strength as well as the concrete contribution depending on the type of shear-reinforced system comprising the slab.

Shear reinforcement consisting of bars or wires and single- or multiple-legs stirrups:

V_c shall not be taken greater than $V_c = 2\lambda\sqrt{f'_c}b_o d$

V_n shall not be taken greater than $V_n = 6\sqrt{f'_c}b_o d$

Shear reinforcement consisting of headed shear studs:

V_c shall not be taken greater than $V_c = 3\lambda\sqrt{f'_c}b_o d$

V_n shall not be taken greater than $V_n = 8\sqrt{f'_c}b_o d$

Note that in all cases $\sqrt{f'_c}$ is limited to 100 psi (0.70 MPa).

A.2 *FIB* MODEL CODE 2010 (MODEL CODE FOR CONCRETE STRUCTURES)

As defined in ACI 318-14, the punching shear strength of a flat two-way slab is assumed to be the summation of the resistance provided by concrete and the resistance provided by shear reinforcement, if present:

$$V_{Rd} = V_{Rd,c} + V_{Rd,s} \qquad \text{(A-7)}$$

$V_{Rd,c}$ = Nominal shear strength provided by concrete.

$V_{Rd,s}$ = Nominal shear strength provided by shear reinforcement.

The design shear resistance attributed to concrete can be estimated as:

$$V_{Rd,c} = k_{\psi} \frac{\sqrt{f_{ck}}}{\gamma_c} b_o d_v \qquad \text{(A-8)}$$

with f_{ck} (compressive cylindrical strength) in [MPa] and d_v taken as the distance from the centroid of the reinforcement layers to the supported area (i.e., shear-resisting effective depth).

The parameter k_{ψ} depends on the rotations of the slab and is expressed as follows:

$$k_{\psi} = \frac{1}{1.5 + 0.9 k_{dg} \psi d_v} \qquad \text{(A-9)}$$

where:

$$k_{dg} = \frac{32}{16 + d_g} \geq 0.75 \qquad \text{(A-10)}$$

The coefficient k_{dg} accounts for aggregate size. Provided that the size of the maximum nominal aggregate particles (e.g. nominal size of coarse aggregates), d_g, is not less than 16mm (5/8in), k_{dg} can be taken as 1.0. For aggregate sizes larger than 16mm, (A-9) may also be used. ψ refers to the rotation of the slab around the supported area (see Figure A.2).

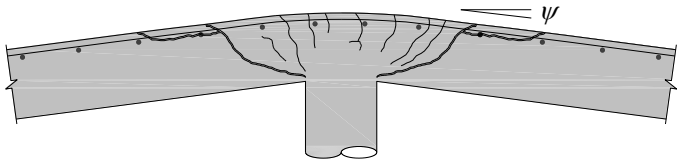

Figure A.2: Rotation (ψ) of a slab (Adapted from *fib* Model Code 2010)

The design shear resistance provided by shear reinforcement may be taken as:

$$V_{Rd,s} = \sum A_{sw} k_e \sigma_{swd} \quad \text{(A-11)}$$

$\sum A_{sw}$ is the sum of the cross-sectional area of all shear reinforcement suitably anchored, or developed, and intersected by the potential failure surface within the zone bounded by $0.35d_v$ and d_v from the edge of the supported area (refer to Figure A.3), and k_e, the coefficient of eccentricity, can be determined as a function of the moment transferred from the column to the slab as:

$$k_e = \frac{1}{1 + e_u / b_u} \quad \text{(A-12)}$$

where e_u is the eccentricity of the resultant of shear forces with respect to the centroid of the basic control perimeter and b_u is the diameter of a circle with the same surface as the region inside the basic control perimeter. σ_{swd} refers to the stress that is activated in the shear reinforcement when is not necessarily equal to the yield stress of the reinforcement and can be estimated as:

$$\sigma_{swd} = \frac{E_s \psi}{6}\left(1 + \frac{f_{bd}}{f_{ywd}}\frac{d_v}{\varphi_w}\right) \leq f_{ywd} \quad \text{(A-13)}$$

where E_s is the modulus of elasticity of steel, f_{ywd} is the yield strength, φ_w denotes the diameter of the shear reinforcement, and the bond parameter, f_{bd} may be taken as 3.0 MPa (0.44 ksi) for corrugated/deformed/ribbed bars.

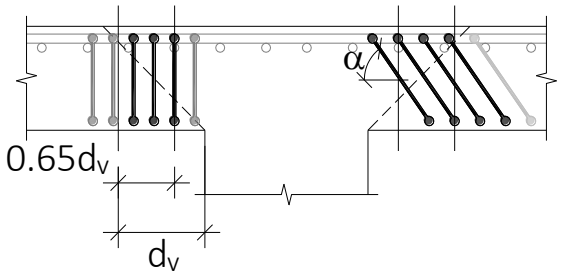

Figure A.3: Shear reinforcement activated at failure (Adapted from *fib* Model Code 2010)

When inclined shear reinforcement or bent-up bars are used, the design resistance provided by shear reinforcement is taken as:

$$V_{Rd,s} = \sum A_{sw} k_e \sigma_{swd} \sin\alpha \qquad \text{(A-14)}$$

$$\sigma_{swd} = \frac{E_s \psi}{6}(\sin\alpha + \cos\alpha)\left(\sin\alpha + \frac{f_{bd}}{f_{ywd}}\frac{d_v}{\varphi_w}\right) \le f_{ywd} \qquad \text{(A-15)}$$

where α denotes the angle between the shear reinforcement and the longitudinal axis of the specimen.

The maximum, or upper limit, punching shear resistance is also checked against the crushing capacity of the concrete struts comprising the supported area:

$$V_{Rd,\max} = k_{sys} k_{\psi} \frac{\sqrt{f_{ck}}}{\gamma_c} b_o d_v \le \frac{\sqrt{f_{ck}}}{\gamma_c} b_o d_v \qquad \text{(A-16)}$$

The coefficient k_{sys} accounts for the performance of punching shear reinforcing systems to control shear cracking, and to suitably confine compression struts at the soffit of the slab. In the absence of other data, a value $k_{sys} = 2.0$ can be used.

To determine the rotation of the slab around the supported area, *fib* Model Code 2010 defines four different approaches, referred to as "level of approximation":

Level 1 approximation (For a regular flat slab designed on the basis of an elastic analysis without significant redistribution of internal forces)

$$\psi = 1.5 \frac{r_s}{d} \frac{f_{yd}}{E_s} \qquad \text{(A-17)}$$

where r_s denotes the position where the radial bending moment is zero with respect to the support axis.

Level 2 approximation (In cases where significant bending moment redistribution is considered in the design)

$$\psi = 1.5 \frac{r_s}{d} \frac{f_{yd}}{E_s} \left(\frac{m_{Ed}}{m_{Rd}} \right)^{1.5} \qquad \text{(A-18)}$$

m_{Ed} is the average moment per unit length for calculation of the flexural reinforcement in the support strip (for the considered direction);

m_{Rd} is the design average flexural strength per unit length in the support strip (for the considered direction).

Level 3 approximation

The coefficient 1.5 specified for levels of approximation 1 and 2 can be replaced by 1.2 if: (1) r_s is calculated using a linear elastic (uncracked) model, and (2) m_{Ed} is calculated from a linear elastic (uncracked) model as the average value of the moment for design of the flexural reinforcement over the width of the support.

Level 4 approximation

The rotation can be calculated on the basis of a nonlinear analysis of the structure accounting for cracking, tension-stiffening effects, yielding of the reinforcement, and other nonlinear effects relevant to providing an accurate assessment of the structure.

A.3 CSCT (CRITICAL SHEAR CRACK THEORY; MUTTONI ET AL., 2009)

Similar to that defined for the ACI 318-14 and *fib* Model Code 2010 provisions:

$$V_{R,in} = V_{Rc} + V_{Rs} \tag{A-19}$$

Muttoni proposed the following failure criterion, which has shown to provide good agreement with a series of 99 punching shear tests of slabs without shear reinforcement:

$$\frac{V_R}{b_0 d\sqrt{f_c}} = \frac{9}{1+15\dfrac{\psi d}{d_{g0}+d_g}} \tag{A-20}$$

where ψ is the rotation of the slab around the support, b_0 is the control perimeter (defined at d/2 beyond the tip of the crack, typically at the face of the column), d is the average effective depth of the member, f_c is the compressive concrete strength (cylinder), d_g is the maximum aggregate size, and d_{g0} is a reference aggregate size set to 16 mm (0.63in.)

The contribution of the shear reinforcement is determined by assuming that the width of the critical shear crack is proportional to the product of the effective depth of the specimen times the rotation of the slab:

$$w = \kappa\psi d \tag{A-21}$$

where κ is a constant whose value is proposed as 0.50.

Assuming that the failure is conical, and that the center of the rotation is located at the tip of the crack, the expressions for the relative displacements of the crack lips

parallel (w_{bi}) and perpendicular (δ_{bi}) to the shear reinforcement can be obtained (see Figure A.4) from the following:

$$w_{bi} = \kappa\psi h_i \cos\left(\alpha + \beta_i - \frac{\pi}{2}\right) \tag{A-22}$$

$$\delta_{bi} = \kappa\psi h_i \sin\left(\alpha + \beta_i - \frac{\pi}{2}\right) \tag{A-23}$$

where h_i denotes the distance between the tip of the crack and the point where the shear reinforcement intersects the critical shear crack, α is the angle of the critical shear crack (assumed to be equal to 45 degrees) and β is the angle between the shear reinforcement and the slab plane.

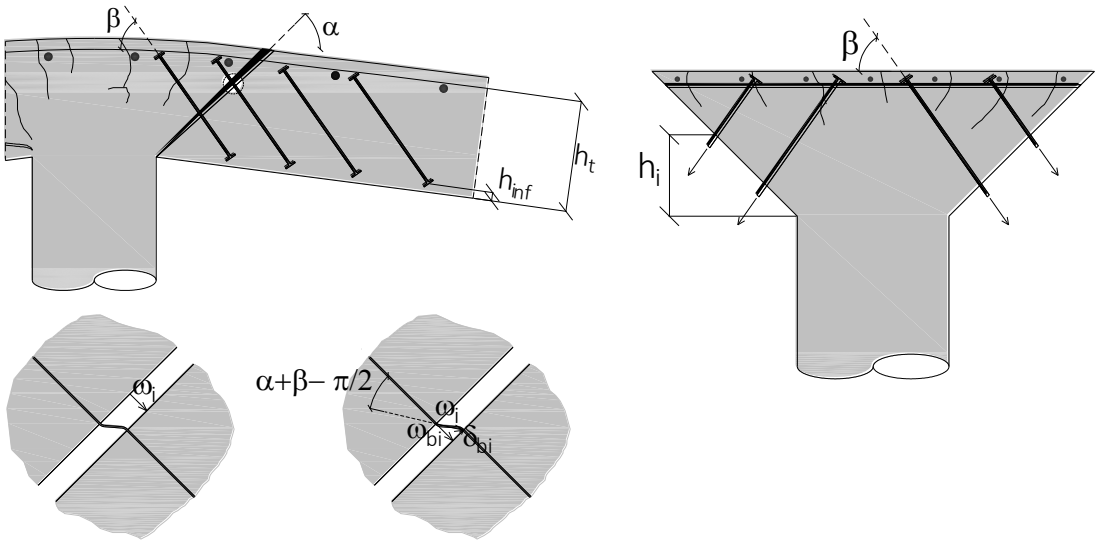

Figure A.4: Contribution of shear reinforcement (Adapted from Muttoni et al., 2009)

Thus, the stress in the shear reinforcement (σ_{si}) is determined by means of w_{bi}. For the case of reinforcing deformed bars, assuming that the bond is activated on both sides of the critical shear crack, and considering a rigid perfectly-elastic bond model, the

following expression for determining the stress in the shear reinforcement is provided by the following:

$$\sigma_{si} = \sqrt{\frac{4\tau_b E_s w_b}{d_b}} \leq f_{yw} \qquad \text{(A-24)}$$

where τ_b is the bond stress (assumed as 3.0 MPa (0.44 ksi)), d_b is the bar diameter, and f_{yw} denotes the yield strength.

With σ_{si}, the shear strength provided by shear reinforcement is computed as:

$$V_s = \sum_{i=1}^{n} \sigma_{si}(\psi) A_{si} \sin\beta_i \qquad \text{(A-25)}$$

A.4 EUROCODE 2 (DESIGN OF CONCRETE STRUCTURES)

The shear resistance should be checked along defined control perimeters. The basic control perimeter u_1 may normally be taken at a distance $2.0d_{eff}$ from the loaded area and should be constructed so that its length be minimized. The effective depth of the slab is assumed constant and is taken as follows:

$$d_{eff} = \frac{d_y + d_z}{2} \qquad \text{(A-26)}$$

where d_y and d_z are the effective depths of the reinforcement in two orthogonal directions.

The design procedure for punching shear is based on checks at a series of control sections, which have a similar shape as the basic control section. The following design shear stresses, per unit area along the control sections, are defined:

$V_{Rd,c}$ = Design value of the punching shear resistance of a slab without shear reinforcement along the control section considered.

$V_{Rd,cs}$ = Design value of the punching shear resistance of a slab containing shear reinforcement along the control section considered.

$V_{Rd,max}$ = Design value of the maximum punching shear resistance along the control section considered.

In estimating the punching shear strength of reinforced concrete flat slabs, the following checks should be performed:

- At the perimeter of the loaded area (i.e. column perimeter), the maximum punching shear stress should not exceeded ($V_{Ed} < V_{Rd,mac}$).
- Shear reinforcement is not needed if the punching shear stress is less than the design value of the punching shear resistance without shear reinforcement ($V_{Ed} < V_{Rd,c}$).
- If the design value of punching shear resistance without shear reinforcement is exceeded, shear reinforcement should be provided.

The punching shear resistance per unit area attributed to a slab without shear reinforcement is given by:

$$V_{Rd,c} = \frac{0.18}{\gamma_c} k(100\rho_1 f_{ck})^{1/3} - 0.10\sigma_{cp} < (0.4 f_{ctd} - 0.10\sigma_{cp}) \quad \text{(A-27)}$$

where f_{ck} and f_{ctd} are the characteristic compressive cylinder strength of concrete at 28 days and the mean value of axial tensile strength of concrete respectively [MPa],

$$k = 1 + \sqrt{\frac{200}{d_{eff}}} \leq 2.0 \quad \text{(A-28)}$$

$$\rho_l = \sqrt{\rho_{ly}\rho_{lz}} \leq 0.02 \quad \text{(A-29)}$$

where ρ_{ly} and ρ_{lz} are the longitudinal reinforcement ratios in x- and y- directions respectively. They should be calculated as mean values considering a slab width equal to the column width plus $3d_{eff}$ each side,

$$\sigma_{cp} = \frac{\left(\sigma_{cy} + \sigma_{cz}\right)}{2} \qquad \text{(A-30)}$$

with σ_{cy} and σ_{cz} defined as normal concrete stresses in the critical section in the y- and z-directions (i.e. prestressing effects, negative in compression) [MPa].

When shear reinforcement is required, it should be calculated in accordance with the following:

$$V_{Rd,cs} = 0.75V_{Rd,c} + 1.5(d_{eff} / s_r)A_{sw} f_{ywd,ef} (1/u_1 d_{eff}) \sin\alpha \qquad \text{(A-31)}$$

where A_{sw} is area of shear reinforcement in each perimeter around the column, S_r denotes the radial spacing of layers of shear reinforcement, α is the angle between the shear reinforcement and the plane of the slab, $f_{ywd,ef}$, effective design strength of the punching shear reinforcement ($f_{ywd,ef} = 250 + 0.25d_{eff} < f_{ywd}$), and d_{eff} is the mean effective depth of the slabs.

Appendix. B Material Properties

B.1 Concrete Properties

For each slab-column connection specimen, several 4 x 8 in. cylinders were tested according to ASTM C39 to determine the concrete compressive strength. Additional cylinders were tested to determine the modulus of elasticity according to ASTM C469, and split tensile strength according to ASTM C496. Lastly, a minimum of two concrete prisms and two "dog bones" corresponding to each slab-column connection were sampled for performing bending tests and for evaluating direct tensile strength of the concrete, respectively.

Table B.1 summarizes the obtained concrete mechanical properties for each slab. In addition, the curves illustrated from Figure B.1 to Figure B.8 present the concrete material property test results corresponding to the compression and modulus of elasticity tests for Slabs 1 to 4.

Table B.1: Mechanical Properties of Concrete

Slab	Specimen	f'_c [a] [psi (MPa)]	Age [Days]	E_c [ksi (MPa)]	ε'_c $x10^{-3}$	f'_t [b] [psi (MPa)]	f_r [c] [psi (MPa)]	f_{ct} [d] [psi (MPa)]
1	1	4,279 (29.5)	107	-	-1.91	428 (2.95)	587 (4.05)	473 (3.26)
	2	3,945 (27.2)		-	-1.51	403 (2.78)	608 (4.19)	420 (2.90)
	3	4,346 (30.0)		4,588 (31633)	-1.77	-	736 (5.07)	447 (3.08)
	4	4,228 (29.2)		5,073 (34977)	-1.66	-	-	-
	5	4,087 (28.2)		4,998 (34460)	-1.68	-	-	-
	Average	4,180 (28.8)		4,890 (33720)	-1.706	416 (2.87)	644 (4.44)	447 (3.08)
2	1	4,051 (27.9)	38	-	-1.44	375 (2.59)	705 (4.86)	454 (3.13)
	2	4,392 (30.3)		-	-1.42	350 (2.41)	703 (4.85)	416 (2.87)
	3	4,112 (28.4)		-	-1.71	385 (2.65)	738 (5.09)	490 (3.38)
	4	4,208 (29.0)		3,703 (25531)	-1.56	-	-	-
	5	4,228 (29.2)		3,660 (25235)	-1.38	-	-	-
	6	4,173 (28.8)		3,797 (26179)	-1.62	-	-	-
	Average	4,190 (28.9)		3,720 (25650)	-1.522	370 (2.55)	715 (4.93)	453 (3.12)
3	1	4,020 (27.7)	25	-	-1.85	399 (2.75)	554 (3.82)	360 (2.48)
	2	3,614 (24.9)		-	-2.29	407 (2.81)	643 (4.43)	306 (2.11)
	3	4,014 (27.7)		-	-1.98	-	622 (4.29)	354 (2.44)
	4	3,898 (26.9)		3,514 (24228)	-1.79	-	-	-
	5	3,984 (27.5)		3,378 (23290)	-1.57	-	-	-
	Average	3,900 (26.9)		3,450 (23790)	-1.896	403 (2.78)	606 (4.18)	340 (2.34)
4	1	2,891 (19.9)	33	-	-1.53	298 (2.05)	589 (4.06)	391 (2.70)
	2	3,177 (21.9)		-	-1.71	324 (2.23)	657 (4.53)	376 (2.59)
	3	3,284 (22.6)		-	-2.22	304 (2.10)	572 (3.94)	399 (2.75)
	4	3,533 (24.4)		3,248 (22394)	-1.30	-	-	-
	5	3,302 (22.8)		3,381 (23311)	-1.44	-	-	-
	6	3,344 (23.1)		3,016 (20794)	-1.27	-	-	-
	Average	3,260 (22.5)		3,220 (22200)	-1.578	309 (2.13)	606 (4.18)	389 (2.68)

[a] Compressive Strength Test (ASTM C39)
[b] Direct Tension Test (No test standard available)
[c] Modulus of Rupture Test (ASTM C78)
[d] Split Tension Test (ASTM C496)

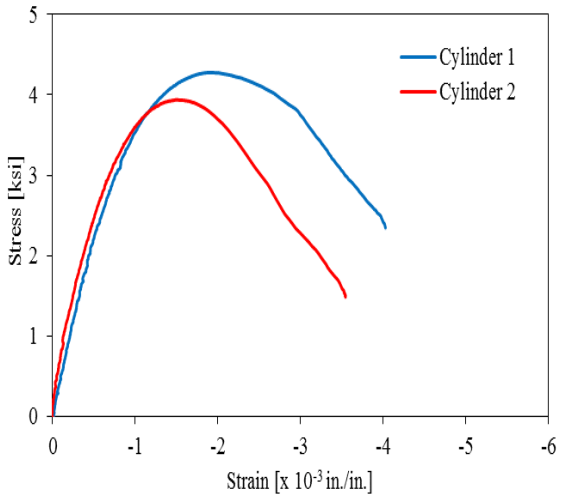

Figure B.1: Compression Test Results; Slab 1

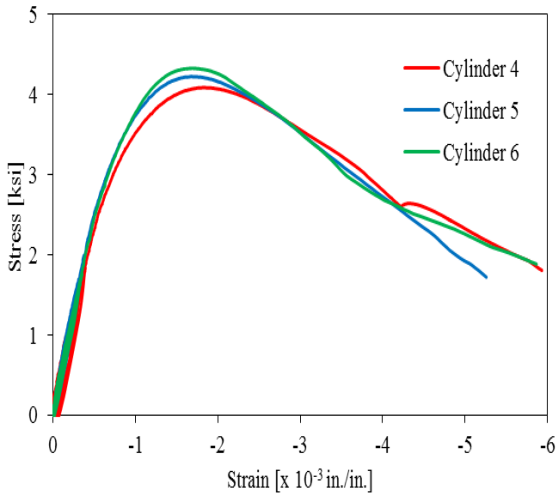

Figure B.2: Modulus of Elasticity Test Results; Slab 1

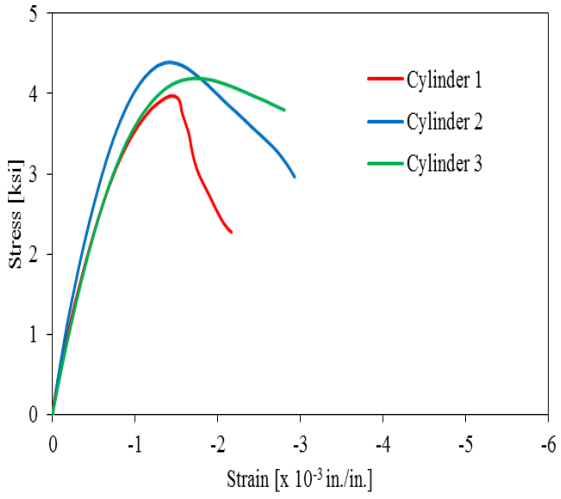

Figure B.3: Compression Test Results; Slab 2

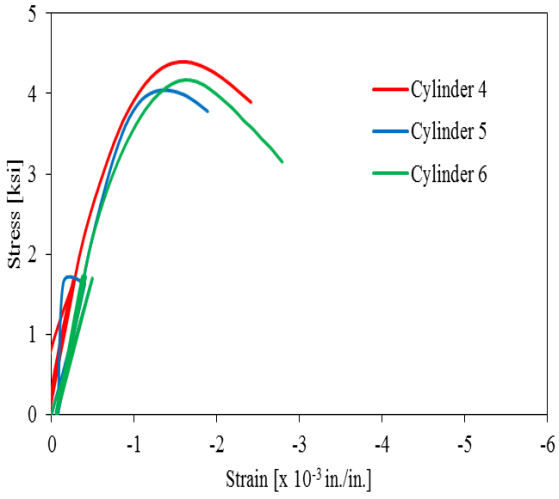

Figure B.4: Modulus of Elasticity Test Results; Slab 2

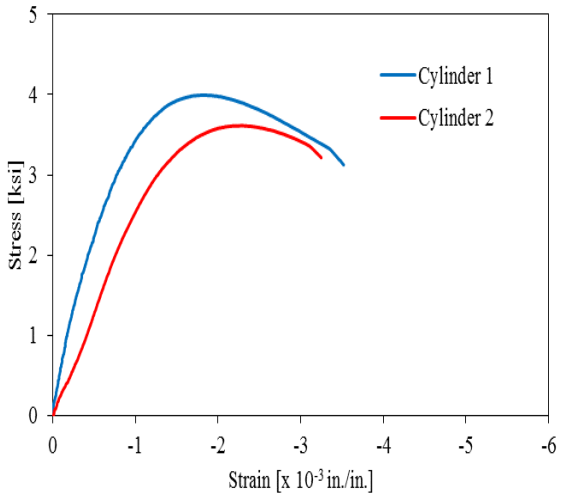

Figure B.5: Compression Test Results; Slab 3

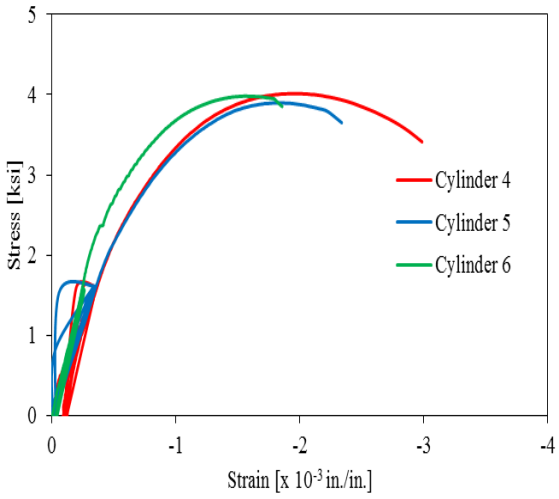

Figure B.6: Modulus of Elasticity Test Results; Slab 3

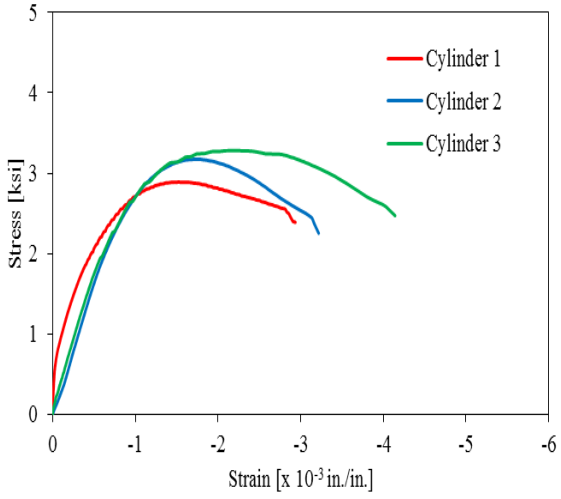

Figure B.7: Compression Test Results; Slab 4

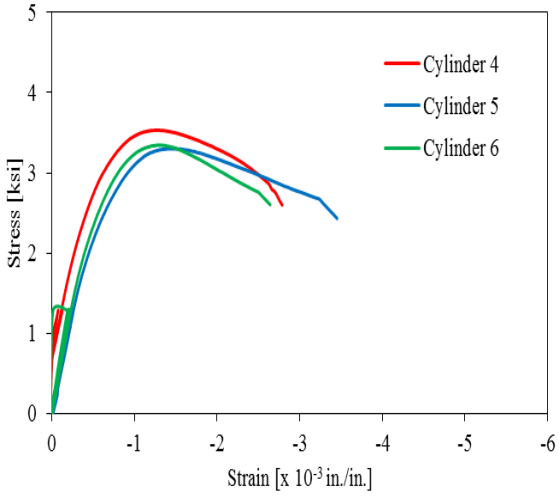

Figure B.8: Modulus of Elasticity Test Results; Slab 4

B.2 COUPON TESTING

Table B.2 and the curves presented from Figure B.9 to Figure B.12 show the mechanical properties of the steel reinforcement used in the experimental program. The average yield strength and average ultimate strength were based on repeatable results of three tests for the weldable bars (i.e., inclined working members) and five tests for the rest of the steel.

Table B.2: Steel Reinforcement Mechanical Properties

Type of Reinforcement	Designation	Coupon	Average Yield Strength [ksi (MPa)]	E_s [ksi (MPa)]	Average Ultimate Strength [ksi (MPa)]
Longitudinal [e]	No.3	1	78.5 (541)	28248 (194763)	121.4 (837)
		2	75.2 (518)	28093 (193694)	117.6 (811)
		3	77.3 (533)	29861 (205884)	122.0 (841)
		4	75.0 (517)	29807 (205512)	117.9 (813)
		5	78.8 (543)	27050 (186503)	122.0 (841)
		Average	77.0 (531)	28610 (197260)	120.1 (828)
	No.7	1	74.0 (510)	28067 (193515)	107.4 (740)
		2	74.9 (516)	28876 (199093)	106.6 (735)
		3	75.2 (518)	27350 (188572)	107.1 (738)
		4	68.6 (473)	26031 (179477)	106.8 (736)
		5	75.0 (517)	27590 (190226)	107.7 (743)
		Average	73.5 (507)	27580 (190160)	107.1 (738)
Shear Studs [f]	½" headed	1	62.5 (431)	31703 (218585)	78.7 (543)
		2	60.7 (419)	30788 (212276)	76.0 (524)
		3	62.0 (427)	30790 (212290)	78.0 (538)
		4	61.5 (424)	30386 (209504)	77.4 (534)
		5	62.4 (430)	29884 (206043)	77.9 (537)
		Average	61.8 (426)	30710 (211740)	77.6 (535)
Shear Inclined Bars [g]	No.3	1	77.5 (534)	23062 (159007)	97.6 (673)
		2	77.4 (533)	31981 (220501)	98.7 (681)
		3	76.3 (526)	32970 (227320)	98.7 (681)
		Average	77.1 (532)	29340 (202290)	98.4 (678)

[e] Grade 60 deformed reinforcing bars
[f] Grade 60 smooth steel studs
[g] Grade 60 weldable deformed reinforcing bars

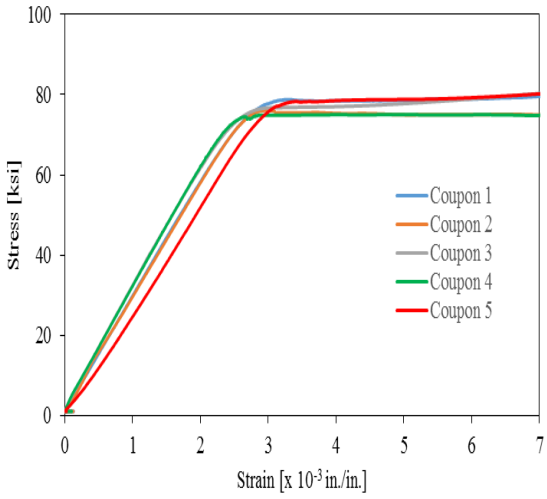

Figure B.9: Strain-Stress Curves for No. 3 coupon tests

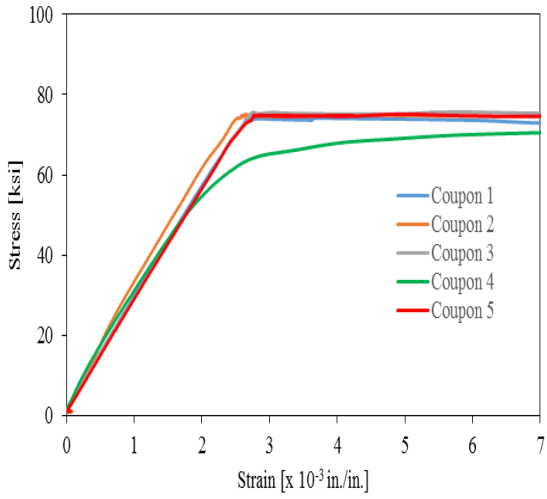

Figure B.10: Strain-Stress Curves for No. 7 coupon tests

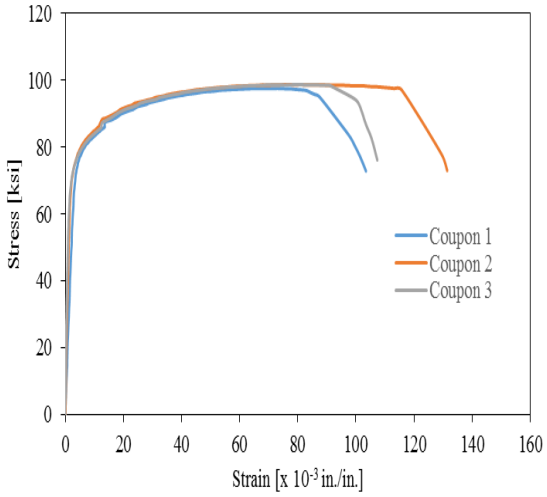

Figure B.11: Strain-Stress Curves for weldable No. 3 coupon tests

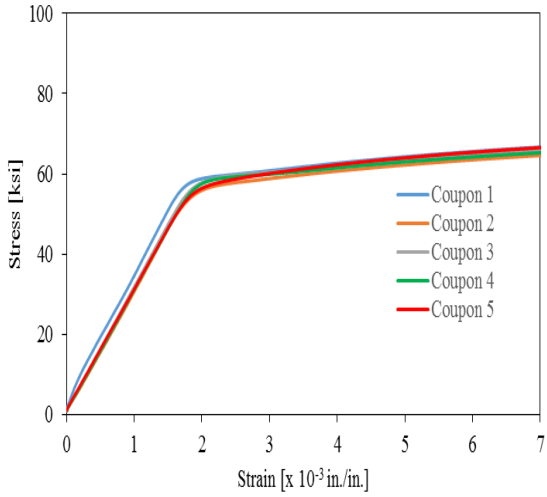

Figure B.12: Strain-Stress Curves for smooth stud coupon tests

Appendix. C Test Photographs

The following figures show the crack development observed in the slabs over the course of testing.

C.1 SLAB 1

Figure C.1: Damage Observed in Slab 1 at V = 100 kips (V/V_U = 20 %)

Figure C.2: Damage Observed in Slab 1 at V = 150 kips (V/V_U = 29 %)

Figure C.3: Damage Observed in Slab 1 at V = 200 kips (V/V_U = 39 %)

Figure C.4: Damage Observed in Slab 1 at V = 250 kips (V/V_U = 49 %)

Figure C.5: Damage Observed in Slab 1 at V = 300 kips (V/V_U = 59 %)

Figure C.6: Damage Observed in Slab 1 at V = 350 kips (V/V_U = 69 %)

Figure C.7: Damage Observed in Slab 1 at V = 400 kips (V/V_U = 78 %)

Figure C.8: Damage Observed in Slab 1 at Failure ($V = V_U = 511$ kips)

C.2 SLAB 2

Figure C.9: Damage Observed in Slab 2 at $V = 100$ kips ($V/V_U = 29$ %)

Figure C.10: Damage Observed in Slab 2 at V = 150 kips (V/V_U = 43 %)

Figure C.11: Damage Observed in Slab 2 at V = 200 kips (V/V_U = 57 %)

Figure C.12: Damage Observed in Slab 2 at V = 250 kips (V/V_U = 71 %)

Figure C.13: Damage Observed in Slab 2 at V = 300 kips (V/V_U = 86 %)

Figure C.14: Damage Observed in Slab 2 at failure (V = V_U = 350 kips)

C.3 SLAB 3

Figure C.15: Damage Observed in Slab 3 at V = 100 kips (V/V_U = 26 %)

Figure C.16: Damage Observed in Slab 3 at V = 150 kips (V/V_U = 39 %)

Figure C.17: Damage Observed in Slab 3 at V = 200 kips (V/V_U = 52 %)

Figure C.18: Damage Observed in Slab 3 at V = 300 kips (V/V_U = 79 %)

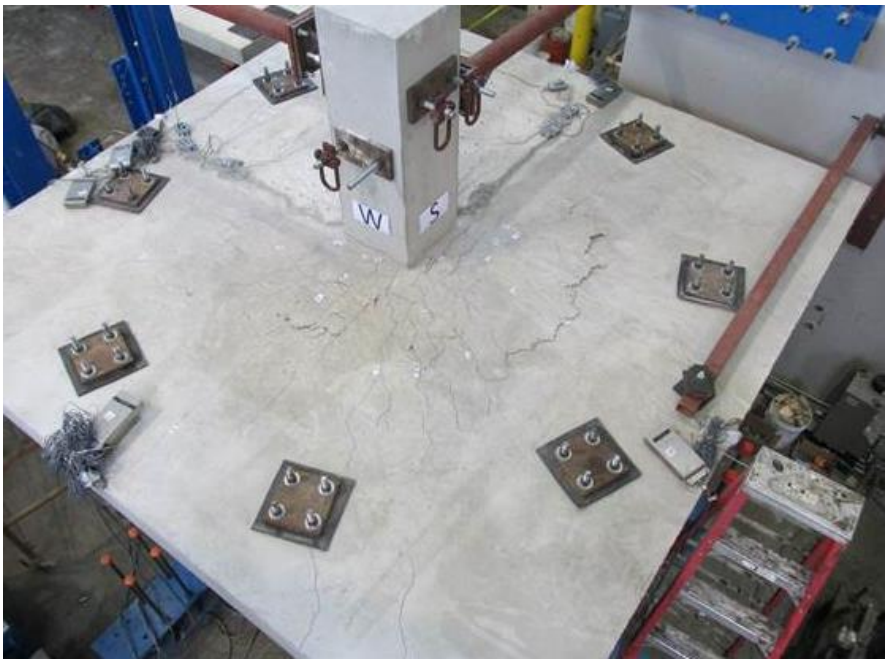

Figure C.19: Damage Observed in Slab 3 at failure (V = V_U = 382 kips)

C.4 SLAB 4

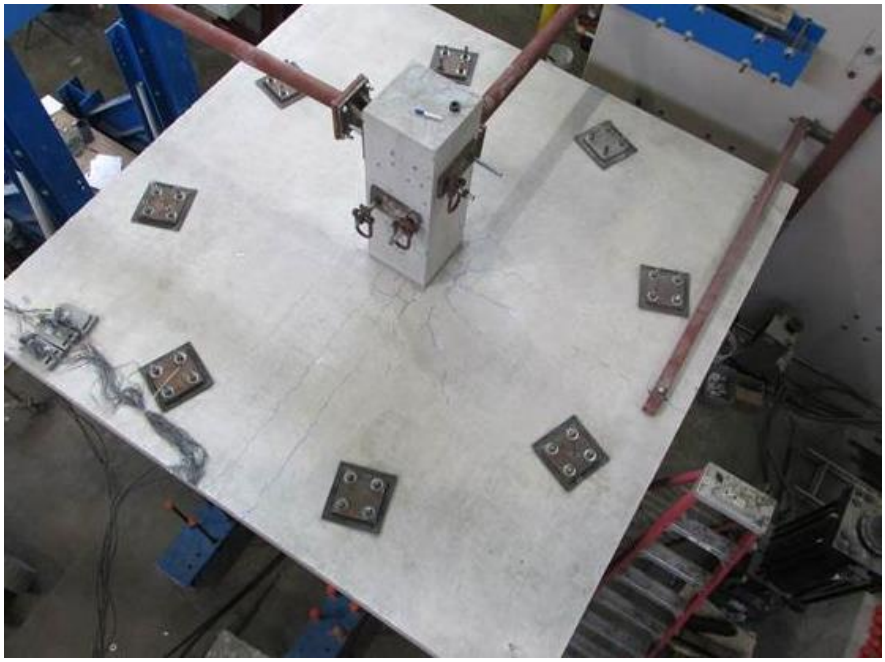

Figure C.20: Damage Observed in Slab 4 at V = 100 kips (V/V_U = 41 %)

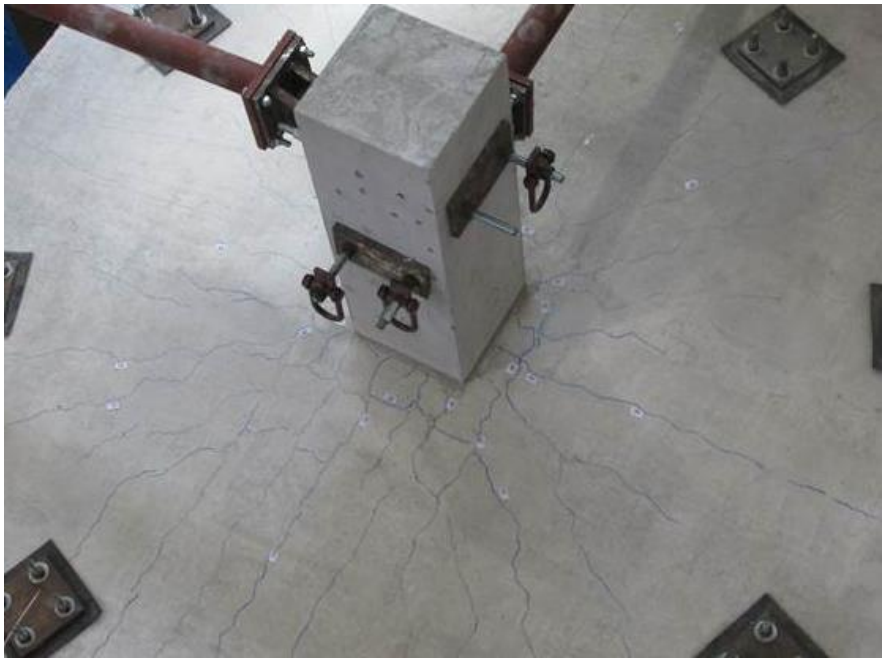

Figure C.21: Damage Observed in Slab 4 at V = 175 kips (V/V_U = 71 %)

Figure C.22: Damage Observed in Slab 4 at V = 200 kips (V/V_U = 81 %)

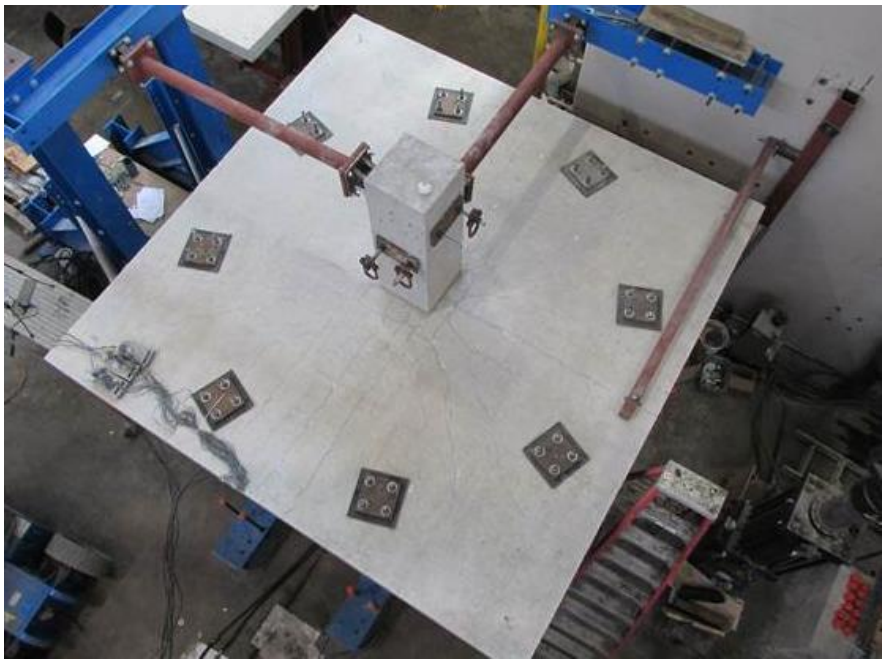

Figure C.23: Damage Observed in Slab 4 at failure ($V = V_U$ = 246 kips)

References

ACI Committee 318 (2014). "318-14: Building Code Requirements for Structural Concrete and Commentary".

Beutel, R. and Hegger, J. (2002). "The Effect of Anchorage on the Effectiveness of the Shear Reinforcement in the Punching Zone", Cement & Concrete Composites 24 (2002), pp. 539-549.

Collins, M.P and Mitchell, D. (1997). "Prestressed Concrete Structures", Response Publications, Toronto and Montreal.

European Committee for Standardization (2004). "Eurocode 2: Design of Concrete Structures".

Fernandez Ruiz, M. and Muttoni, A. (2009). "Applications of Critical Shear Crack Theory to Punching of Reinforced Concrete Slabs with Transverse Reinforcement", ACI Struct. J., V 106(4), Jul-Aug, pp. 485-494.

Fernandez Ruiz, M., Muttoni, A., and Kunz J. (2010). "Strengthening of Flat Slabs Against Punching Shear Using Post-Installed Shear Reinforcement", ACI Struct. J., V. 107(4), Jul-Aug, pp. 434-441.

International Federation for Structural Concrete (*fib*) (2010). "The *fib* Model Code for Concrete Structures 2010".

Mitchell, D. and Cook, W. (1984). "Preventing Progressive Collapse of Slab Structures". ASCE Journal of Structural Engineering, 110 (7), pp. 1513-1532.

Muttoni, A., Fernandez Ruiz, M., Bentz E., Foster S., and Sigrist V. (2013). "Background to *fib* Model Code 2010 Shear Provisions – Part II: Punching Shear", Structural Concrete 14 (2013), No. 3, pp. 204-214.

Oliveira, D.R., Melo, G.S., and Regan, P.E. (2000). "Punching Strengths of Flat Plates with Vertical or Inclined Stirrups", ACI Struct. J., V. 97(3), May-June, pp. 485-491.

Richart, F.E. (1927). "An Investigation of Web Stresses in Reinforced Concrete Beams", University of Illinois. Engineering Experimental Station. Bulletin No. 166, pp. 7-103.

Vita

Mario Glikman was born in Buenos Aires, Argentina on January 15, 1987 to Jose Mario Glikman and Ana Maria Falco. After completing his 6-year bachelor's degree with professional certification in civil engineering at Universidad Católica Argentina and working as a structural engineer for almost five years, he was awarded an Argentinean Presidential Fellowship in Science and Technology. One year later, he entered the Graduate School at The University of Texas at Austin, where he received his Master of Science in Engineering's degree (Structural Engineering Concentration) in May, 2016.

Email address: marioglikman@gmail.com

This thesis was typed by the author.